LIMNOLOGY
and
OCEANOGRAPHY

ASLO

Limnol. Oceanogr. 9999, 2020, 1–16

doi: 10.1002/lno.11440

Effects of ocean climate on spatiotemporal variation in sea urchin settlement and recruitment

Daniel K. Okamoto ,[1,2*] **Stephen C. Schroeter,**[3] **Daniel C. Reed**[3]

[1]Department of Biological Science, Florida State University, Tallahassee, Florida
[2]Ecology, Evolution and Marine Biology, University of California Santa Barbara, Santa Barbara, California
[3]Marine Science Institute, University of California Santa Barbara, Santa Barbara, California

Abstract

Sea urchins are voracious herbivores that influence the ecological structure and function of nearshore ecosystems throughout the world. Like many species that produce planktonic larvae, their recruitment is thought to be particularly sensitive to climatic fluctuations that directly or indirectly affect adult reproduction and larval transport and survival. Yet how climate alters sea urchin populations in space and time by modifying larval recruitment and year-class strength on the time-scales that regulate populations remains understudied. Using a, spatially replicated weekly-biweekly data set spanning 27 yr and 1100 km of coastline, we characterized seasonal, interannual, and spatial patterns of larval settlement of the purple sea urchin (*Strongylocentrotus purpuratus*). We show that large spatial differences in temporal patterns of larval settlement were associated with different responses to fluctuations in ocean temperature and climate. Importantly, we found a strong correlation between larval settlement and regional year class strength suggesting that such temporal and spatial variation in settlement plays an important role in controlling population dynamics. These results provide strong evidence over extensive temporal and spatial domains that climatic fluctuations shape broad-scale patterns of larval settlement and subsequent population structure of an important marine herbivore known to control the productivity, community state, and provisioning services of marine ecosystems.

Large-scale climate oscillations (e.g., El Niño Southern Oscillation, North Atlantic Oscillation) lead to changes in ocean temperature, biogeochemistry, and the severity and frequency of disruptive events that affect ocean circulation, upwelling, and primary productivity (Mantua et al. 1997; Cai 2014). Such shifts impose wide-reaching ecological impacts, in part by altering animal recruitment and food web structure in space and time (Sydeman et al. 2015). Hence, understanding how climate variability alters the recruitment of marine species is particularly important for effective conservation and management of the ocean's resources. Climatic fluctuations give rise to shifts in numerous factors that shape both adult reproduction and larval supply, including primary productivity, temperature, and advection and transport. Given these multiple direct and indirect effects of climate on recruitment, significant challenges remain in achieving such understanding for benthic species with planktonic larvae due to the substantial effort needed to characterize spatial and temporal variation in larval settlement and the numerous sensitive vital rates that contribute to it.

For benthic species like sea urchins, understanding causes and consequences of recruitment variability has both ecological and economic implications. Sea urchin grazing can alter the structure of some of the world's most diverse and productive marine ecosystems, including coral reefs (Edmunds and Carpenter 2001), seagrass meadows (reviewed by Valentine and Heck 1999), and kelp forests (reviewed by Filbee-Dexter and Scheibling 2014). In addition, sea urchins form the basis of important nearshore fisheries in many regions of the world (e.g., Kato and Schroeter 1985; Andrew et al. 2003). As a result, climate-driven changes in sea urchin populations have the potential to profoundly affect the ecological structure and functioning of marine ecosystems and the economic value of the fisheries that they support. Much of the research on controls of sea urchin population dynamics has focused on the roles of predation and disease in controlling adult abundance and their cascading influence on community structure (e.g., Estes and Duggins 1995; Lafferty 2004; Filbee-Dexter and Scheibling 2014; Burt et al. 2018). Yet short-term empirical

*Correspondence: dokamoto@bio.fsu.edu

Additional Supporting Information may be found in the online version of this article.

Author Contribution Statement: D.K.O., S.C.S., and D.C.R. designed research. D.K.O. designed, built, and conducted analyses and wrote the initial manuscript. D.K.O., D.C.R., and S.C.S. managed data. S.C.S. initiated and oversaw data collection and collaborated on all analyses. All authors contributed to revisions.

studies (months to a few years) suggest that environmentally regulated larval supply is likely an important driver of adult urchin dynamics (Ling et al. 2009; Hernández et al. 2010). Despite the widespread recognition of the importance of recruitment variation in controlling population fluctuations in many marine species (Shelton and Mangel 2011), relatively few studies have examined the biotic and abiotic processes controlling the supply of sea urchin larvae in nature (but see Ling et al. 2009; Hernández et al. 2010), and the degree to which they affect the abundance and dynamics of older life stages over time scales that impact population dynamics.

Fluctuations in climate can affect spatial and temporal patterns of larval supply by influencing the production of larvae by benthic adults, transport of larvae to adjacent habitats, and the survival of larvae in the plankton. Increases in ocean temperature can impact larval production by: (1) increasing adult mortality via the spread of water-borne pathogens (reviewed by Feehan and Scheibling 2014) and (2) reducing adult fecundity and inhibiting gametogenesis by altering food quantity and quality (Cochran and Engelmann 1975; Basch and Tegner 2007; Okamoto 2014; Foster et al. 2015). Because sea urchins produce feeding larvae that spend weeks to months in the plankton, increases in ocean temperature can also affect larval development, growth, and survival, either directly or indirectly by altering the availability of their phytoplankton food source (Strathmann 1987; Hoegh-Guldberg and Pearse 1995; Bertram and Strathmann 1998; Byrne et al. 2009). Finally, climate-related changes in patterns of ocean circulation can affect the transport of larvae from source to destination (but see Siegel et al. 2008; Morgan 2014). Thus, the effects of climatic change on sea urchin recruitment represent cumulative impacts on adult abundance and reproduction, complex current patterns that transport larvae, behavioral responses of larvae, and larval development and survival. Because patterns of ocean temperature, circulation, and upwelling can vary dramatically in space, the effects of climate oscillations on sea urchin recruitment potentially vary over large spatial scales. A dearth of long-term, high-frequency, spatially extensive data has prevented characterizing temporal and spatial variability in larval settlement in sea urchins, the degree to which it is explained by different sources of environmental variation, and the relative importance of these drivers in accounting for fluctuations in population size.

Here we analyzed a 27-yr weekly to biweekly time series of the recruitment of newly metamorphosed larvae (hereafter referred to as larval settlement) at sites distributed across 1100 km of coast in California to investigate sources of spatial and temporal variability in larval settlement of the purple sea urchin *Strongylocentrotus purpuratus*. Our objectives were to: (1) quantify variation in larval settlement across different temporal and spatial scales; (2) evaluate whether larval settlement on artificial substrates predicts year-class strength in natural populations; and (3) determine the relative importance of adult abundance, larval and adult food supply, sea surface temperature (SST), and broad-scale fluctuations in ocean climate in contributing to the observed variation in larval settlement.

Study system

Populations of the purple sea urchin (*S. purpuratus*) occupy shallow subtidal and intertidal rocky substrata from at least 27°N on the western coast of the Baja Peninsula (Olivares-Bañuelos et al. 2008) to at least 59°N on the Kenai Peninsula in Alaska (Field and Walker 2003). Purple urchins are broadcast spawners and the seasonality of their spawning is generally thought to be driven by spring photoperiod and temperature (Gonor 1973; Cochran and Engelmann 1975; Pearse et al. 1986). Energy available for gonad production is largely determined by macroalgal food availability; specifically, sea urchins in barrens devoid of abundant macroalgae can show dramatic reductions in fecundity (> 99%), and resumption of feeding in emaciated urchins can lead to gonadal recovery within 2–3 months (Okamoto 2014). Results from the field and laboratory indicate that the thermal upper limit to completion of gametogenesis is about 17°C (Cochran and Engelmann 1975; Basch and Tegner 2007). Fertilized zygotes develop into planktonic echinoplutei larvae that feed exclusively on phytoplankton (Strathmann 1987). After spending several weeks to months in the plankton, individuals begin final metamorphosis and settle to the benthos (Strathmann 1978) at a size of ~ 500 μm in diameter (Okamoto unpubl. data). Larval settlement varies dramatically among locations at both small and large spatial scales (Ebert 2010). Once settled, fully competent individuals occupy cobble and other complex substrata and between 12 and 24 months become visible in benthic surveys at 1–2 cm diameter. For a full review, see Rogers-Bennett and Okamoto (2020).

Collection of newly settled urchins along the coast of California, U.S.A. (1990–2016)

Settlement of newly metamorphosed purple sea urchins was sampled in three major regions along the California coast from 1990 through 2016, with a total of 54,588 replicate observations. Sampling regions (from south to north) included two sites in San Diego County (Scripps Pier and Ocean Beach Pier), four sites in the Santa Barbara Channel (Anacapa Island, Stearns Wharf, Ellwood Pier, and Gaviota Pier), and one site at Point Cabrillo in Fort Bragg (Fig. 1). San Diego and the Santa Barbara Channel lie within the Southern California Bight and Fort Bragg is in northern California. At each site, newly settled urchins were collected using nylon-bristled scrub brushes (2.5 cm long bristles and a 6×9 cm wooden base) suspended 1–2 m from the benthos (Ebert et al. 1994). The majority of deployments included 4–8 replicate brushes collected weekly at each site from 1990 to 2003, and biweekly thereafter through 2016. Upon collection brushes were transported to the laboratory in plastic bags and rinsed through a 350 μm mesh sieve. Purple urchins were sorted from other species, counted, and preserved. A more detailed description of the

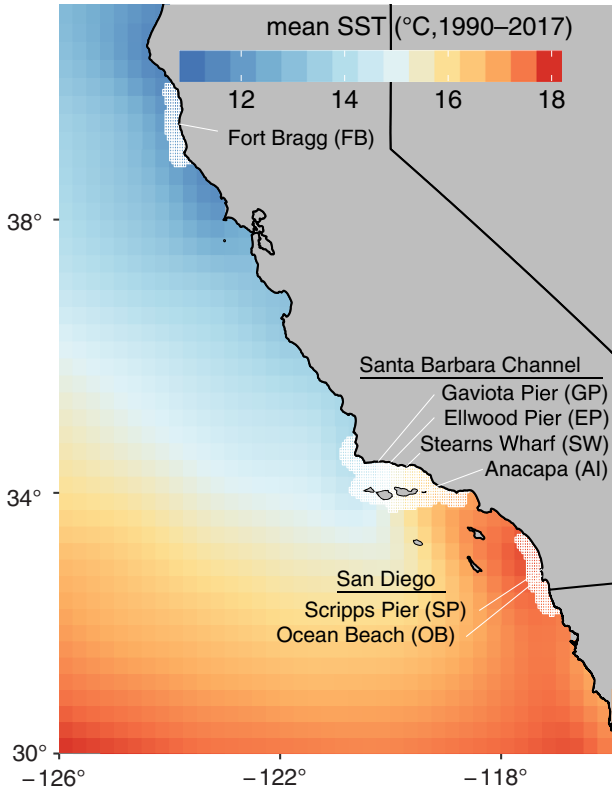

Fig. 1. Map of larval settlement collection sites in California. Colors represent the average spatial gradient of SST from 1991 to 2017. The hatched white lines show the shoreline buffer used to constrain SST and sea surface chlorophyll index to local larval settlement observations.

sampling methods, geographic and taxonomic coverage, and links to the data and metadata are provided in Schroeter et al. (2019).

Methods

Spatiotemporal trends in larval settlement

We estimated seasonal, annual, and spatial patterns in larval settlement using an integrated spatiotemporal Bayesian model that accounted for the spatially and temporally intercorrelated and heterogeneous nature of the multivariate time series. We used a Bayesian state-space formulation for the model for several reasons. First, episodic periods of low replication, low observation numbers, missing data, or slight variation in the sampling interval mean that the true number of settlers may not be reflected in the empirical mean value from brush data (i.e., the true value is not always observable). Second, when brushes contained hundreds or more individual urchins, species identification consisted of subsampling urchins to estimate proportions of individual species (in this case *S. purpuratus* vs. the rarer red urchin, *Mesocentrotus franciscanus*). This subsampling routine requires accounting for the uncertainty in the sampled species ratios in the estimation of settler abundance, which we did by incorporating a Bayesian prior in the form of a Beta distribution with hyperparameters as the observed ratio and total subsample count (the Jeffrey's prior for ratios from binomial counts). Third, initial examination of the data indicated substantial seasonal and interannual variability that was multiplicative among-samples within each period, as well as serial autocorrelation and spatial components that needed to be simultaneously accounted for.

We used a Poisson observation likelihood to link the biweekly mean estimate from the trend equation ($\hat{\mu}_{t,s}$ —*see* Table 1, Eqs. 3, 4, and Table 2) to observed counts of larval settlers (N) for each brush (b) within each site (s) within each time interval (t). To account for the above described nuances of the data, we estimated biweekly settlement density ($\hat{\mu}_{t,s}$) as the sum of a site-specific mean ($\beta_{0,s}$), log annual trend ($\text{Annual\_Trend}_{t,s}$), log seasonal trend ($\text{Seas\_Trend}_{t,l}$), and a spatially correlated lognormal process error ($\varepsilon_{t,s}$):

$$\ln \hat{\mu}_{t,s} = \beta_{0,s} + \ln \text{Annual\_Trend}_{t,s} + \ln \text{Seasonal\_Trend}_{t,s} + \varepsilon_{t,s} \quad (1)$$

We estimated trends on the log-scale so that process errors, and seasonal and interannual trends were multiplicative and strictly positive on the original scale.

The annual trends were assumed to be correlated in both space and time, where spatial and temporal covariances were assumed to be independent. The annual spatial covariance was assumed to be unstructured (i.e., no formal distance decay structure) because we only had seven sites. The annual temporal covariance was determined by a Matérn 3/2 kernel because it provided sufficient flexibility to capture interannual trends. The seasonal trend (log-scale) within each site was estimated using a seasonal periodic temporal kernel within the model to capture the cyclical nature of seasonality. The process error ($\varepsilon_{t,s}$) was modeled with an unstructured spatial covariance to account for correlations among sites in their deviations from model expectations. We estimated the model posteriors using Stan (Carpenter et al. 2016) with three 1000 iteration chains after a 1000 iteration burn-in. Stan model code is provided in the Supporting Information. For model equations and symbology, see Tables 1, 2.

Relationship between benthic year-class strength and larval settlement

If year class strength of sea urchins is limited by larval supply, then we should see increases (decreases) in the abundance of juveniles in years following anomalously high (low) larval settlement. We therefore tested whether larval settlement in the Santa Barbara Channel (mean of Anacapa, Stearns Wharf, Ellwood Pier, and Gaviota Pier) was predictive of subsequent juvenile recruitment (hereafter referred to as "year-class strength") on natural reefs in the region. We calculated densities of juveniles (< 2 cm test diameter) from the Channel Islands Kelp Forest Monitoring (KFM) Program (Kushner et al. 2013), including only the nine

Table 1. Equations for the multivariate spatiotemporal models. Variables, parameters, and priors are described in Table 2. Note that there are two primary model forms: a trend estimation model and a Bayesian regression model. Equations apply to both model forms except where specified.

Eq. no.	Description	Equation
3	Total count likelihood	$\begin{cases} \text{Tot}_{t,s,b} \sim \text{Poisson}\left(\hat{\mu}_{t,s} \times D_{t,s,b}/p_{t,s,b}\right) & \text{when subsampled} \\ N_{t,s,b} \sim \text{Poisson}\left(\hat{\mu}_{t,s} \times D_{t,s,b}\right) & \text{otherwise} \end{cases}$
4	Subsampling prior	$p_{t,s,b} \sim \text{beta}(N_{t,s,b} + 0.5,\ NO_{t,s,b} + 0.5)$ when subsampled
5	Prior seasonal temporal correlation function	$\bar{r}_{<t_i,t_j>} = \exp\left[-\frac{2}{1.5^2}\left(0.5 - 0.5\cos\left(\pi\left\|t_i - t_j\right\|\right)\right)\right]$ Periodic Kernel (MacKay 1998)
6†	Prior annual temporal correlation function	$\bar{\bar{r}}_{<t_i,t_j>} = \left(1 + 3^2\right)\left\|t_i - t_j\right\| \exp\left(-3^2\left\|t_i - t_j\right\|\right)$ Matern 3/2 Kernel (Rasmussen and Williams 2006)
7	Prior seasonal spatiotemporal covariance function (separable)	$\bar{\boldsymbol{\Sigma}} = \bar{\boldsymbol{\Omega}} \otimes \left[\bar{\boldsymbol{\sigma}}\,\bar{\mathbf{R}}\right]$
8†	Prior annual spatiotemporal covariance function (separable)	$\bar{\bar{\boldsymbol{\Sigma}}} = \bar{\bar{\boldsymbol{\Omega}}} \otimes \left[\bar{\bar{\boldsymbol{\sigma}}}\,\bar{\bar{\mathbf{R}}}\right]$
9	Matrix of seasonal trends	$\textbf{Seasonal} \sim \text{MVN}(0, \bar{\boldsymbol{\Sigma}})$
10†	Matrix of annual trends	$\textbf{Annual} \sim \text{MVN}(0, \bar{\bar{\boldsymbol{\Sigma}}})$
11a*	First-order autoregressive model	$\boldsymbol{\epsilon}_t = \phi\epsilon_{t-1} + e_t\sqrt{1-\phi^2}$
11b	Spatially correlated process error	$\boldsymbol{e}_t \sim \text{MVN}(0, \sigma\boldsymbol{\Omega})$

*Bayesian regression model only.
†Trend estimation model only.

sites with time series extending from 1990 through 2016. We examined the relationship between larval settlement and year-class strength using a generalized linear mixed effects model (GLMM) with a negative binomial likelihood (a Poisson likelihood indicated overdispersion) and survey site as a random effect. We tested the hypothesis of no correlation using a

Table 2. Definition of parameters, variables, and priors for equations described in Table 1.

Symbol	Description	Type	Prior/input
$\hat{\mu}_{t,s}$	Expected settlement density (per brush, per day) of purple urchins, defined in Eqs. 1 or 2 in the main text for each model.	Estimated	Eqs. 1, 2
$N_{t,s,b}$	Number of purple urchins counted at time *t*, site *s*, and brush *b*. When urchin species within brushes are subsampled, data produced are a total urchin count ($\text{Tot}_{t,s,b}$), a total subsample count of other urchins ($NO_{t,s,b}$), and a purple urchin subsample count ($N_{t,s,b}$).	Input	Data
$\text{Tot}_{t,s,b}$	Total number of urchins counted at time *t*, site *s*, and brush *b*	Input	Data
$p_{t,s,b}$	Estimated proportion of purple urchins in the counts given the subsample (when urchin counts in brushes are subsampled).	Estimated	Eq. 4
$D_{t,s,b}$	Exact number of days of the brush deployment	Input	Data
$\mathbf{X}$	Covariate design matrix—for estimation model represents only site indices, for regression model includes covariates	Input	Data
β	Vector of site-specific scale parameters and covariate coefficients	Estimated	**Scale parameters**: Student *t*: Scale = 2; **Coefficients**: regularized horseshoe prior (*see* "Methods" section).
ϕ	Vector of site-specific first order autoregressive parameters and estimated (regression model only)	Estimated	Uniform −0.95 to 0.95
$\boldsymbol{\Omega}, \bar{\boldsymbol{\Omega}}, \bar{\bar{\boldsymbol{\Omega}}}$	Spatial correlation matrices for process error, annual trends, and seasonal trends (estimated through the Cholesky factor)	Estimated	LKJ prior: Scale = 2 (Lewandowski et al. 2009)
$\bar{\boldsymbol{R}}, \bar{\bar{\boldsymbol{R}}}$	Temporal correlation matrices for annual and seasonal Gaussian processes	Input	Eqs 5, 6
$\boldsymbol{\sigma}, \bar{\boldsymbol{\sigma}}, \bar{\bar{\boldsymbol{\sigma}}}$	Site-specific standard deviation for process error, annual trends, and seasonal trends	Estimated	Half-cauchy: Scale = 2.5 (Polson and Scott 2012)

likelihood ratio test comparing the models that do vs. do not include settlement as a covariate. Models were estimated using glmmTMB (Magnusson et al. 2017) in R (*see* Supporting Information for further details).

Relationships between larval settlement and biotic and abiotic conditions

We estimated the strength of relationships between biweekly larval settlement and various hypothesized physical and biological drivers using an integrated regression model that included a regularized regression within a Bayesian time-series modeling framework (Fig. 2). We used a Poisson observation likelihood to link estimated latent trends $\hat{\mu}_{t,s}$ to the settlement count observations (*see* Table 1, Eqs. 3, 4, and Table 2). We estimated the log biweekly density ($\ln \hat{\mu}_{t,s}$) as a function of the centered and standardized covariates (denoted by the vector $\boldsymbol{x_{t,s}}$) while directly estimating and accounting for seasonal trends (Seasonal_Trend$_{t,s}$), and a separable spatially and temporally correlated, multivariate lognormal process error ($\varepsilon_{t,s}$):

$$\ln \hat{\mu}_{t,s} = \beta_{0,s} + [x_{t,s}]'\beta_s + \ln \text{Seasonal\_Trend}_{t,s} + \varepsilon_{t,s} \qquad (2)$$

We assumed the temporal correlation in the process error $\varepsilon_{t,s}$ followed a first-order autoregressive model.

Because these analyses were correlative, we focused on unbiased parameter estimation rather than hypothesis testing or model comparison per se. We estimated two separate models: one included all locally measured (i.e., for a given site) environmental variables and the other included a common set of composite indices of oceanographic climate ("global covariates"—El Niño Southern Oscillation [ENSO] Index, Pacific Decadal Oscillation [PDO], North Pacific Gyre). Because inclusion of numerous covariates can cause overfitting that leads to bias and uncertainty in the explanatory power of the covariates, we erred on the side of sparsity and assigned the vector of regression coefficients ($\boldsymbol{\beta_l}$) a regularized horseshoe prior (i.e., the Finnish Horseshoe). Sparsity in this case assumed that only a few of the covariates were meaningful without a priori knowledge of which covariates were relevant and which were not. A sparse regression encoded this assumption to allow the data to inform which covariates were relevant and how they were correlated with the response variable. The Finnish horseshoe prior is a Bayesian version of the lasso (Carvalho et al. 2010; Piironen and Vehtari 2017) that produced a data-driven reduction in the influence of weaker covariates by regularization of those coefficients given the data. For full details and model equations, see Tables 1, 2.

Below are the covariates used in the integrated regression model.

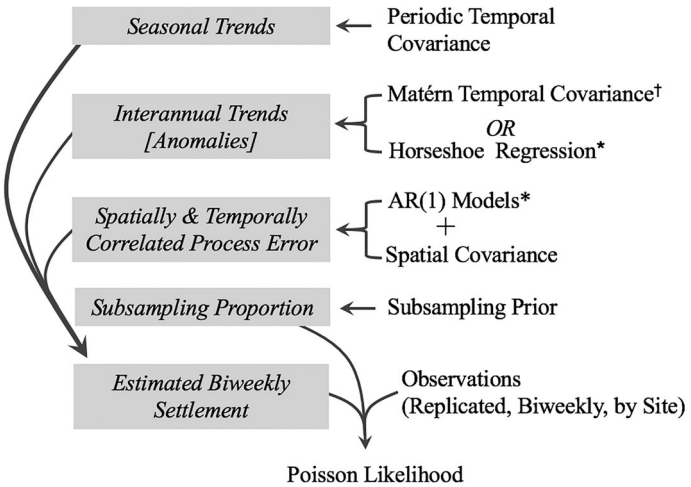

Fig. 2. Diagram of the model structure using either a Matérn temporal covariance (trend estimation model) or a horseshoe regression (correlation estimation model) to estimate anomalies from the mean seasonal trend. For details, see Tables 1, 2. *Bayesian regression model only. †Trend estimation model only.

Oceanographic climate indices (monthly, 1990–2016, all sites)

We used three major global indices of oceanographic climate: the multivariate El Niño Southern Oscillation Index (MEI), the PDO (Mantua and Hare 2002), and the North Pacific Gyre Oscillation (NPGO—Di Lorenzo et al. 2008). The MEI provides a metric of the intensity of ENSO fluctuations, which persist for 6–18 months and explains much of the oceanographic variability in the tropics (Wolter and Timlin 1993, 1998; Di Lorenzo et al. 2013). In contrast, the PDO and NPGO exhibit longer-period fluctuations, explain much of the oceanographic variability in higher latitudes, and the low frequency variability of these metrics are shaped through ENSO forcing of the Aleutian Low and the North Pacific Oscillation, respectively (Di Lorenzo et al. 2013).

Coastal upwelling index (monthly, 1997–2016, all sites)

The Bakun index (Bakun 1973) provides an index of large-scale coastal upwelling and specifically describes the volume of water that is transported offshore from Ekman transport (http://www.pfeg.noaa.gov/ - sites = 33 N–119 W and 39 N–125 W). This index has been used as a large-scale proxy for processes that may favor larval retention and advection from shore in addition to its value as a predictor of coastal productivity (Shkedy and Roughgarden 1997; Wing et al. 2003; Menge et al. 2011; Menge and Menge 2013). We emphasize that this index is not a location-specific metric nor does it consider fine-scale nearshore hydrodynamic processes that are also likely to affect larval retention (Shanks and Eckert 2005; Morgan et al. 2009, 2016, 2018; Shanks and Shearman 2009; Fisher et al. 2014; Shanks et al. 2017; Shanks and Morgan 2018) which remain outside the scope of this study, but worthy of investigation as drivers of settlement trends. Rather we include the Bakun index as an indicator of broader scale coastal upwelling that may affect regional trends in larval supply (e.g., Roughgarden et al. 1988).

Sea surface chlorophyll (monthly, 1997–2016, all sites)

Satellite imagery of sea surface chlorophyll *a* (Chl *a*) provides a spatially and temporally resolved estimate of phytoplankton biomass (mg m^{-3}) that is not available from in situ sampling. We used version 3.1 of the OC-CCI merged ocean color time series (Sathyendranath et al. 2018) that combines SeaWIFs, MERIS, MODIS, and VIIRS to provide the temporal and spatial coverage required for this study. For each larval settlement collection site, we aggregated data into a 30-d moving average (30 d prior to brush collection) for an area 10 km from shore that stretched 150 km alongshore (the average Lagrangian estimate for dispersal distances for species with a planktonic larval duration (PLD) of 30-d; but see Siegel et al. 2003; Shanks 2009). For the site at Anacapa Island, we included any point within a 150 km radius and within 10 km of any coastline. We used 30-d moving averages for chlorophyll and temperature (below) because larvae were exposed to these conditions for at least 30 d prior to settlement, and because averaging over 30 d minimized the effects of serial autocorrelation in the data.

SST (monthly, 1997–2016, all sites)

We used the 30-d moving average of SST, derived from Pathfinder AVHRR (Reynolds et al. 2007) (advanced very high resolution radiometer) that was optimally interpolated at daily and 0.25° latitude/longitude resolution. We spatially aggregated data in the same way as sea surface chlorophyll.

Fall kelp canopy biomass (annual, 1996–2016, Santa Barbara Channel and San Diego only)

Giant kelp (*Macrocystis pyrifera*) is a preferred food and a major constituent of *S. purpuratus* diets in southern California (Foster et al. 2015). The regional biomass of giant kelp *Macrocystis pyrifera* can fluctuate dramatically from year to year (Bell et al. 2015) and cause orders of magnitude variations in *S. purpuratus* fecundity (Okamoto 2014). We estimated intra- and interannual variability in the biomass of giant kelp from Landsat Thematic Mapper satellite imagery (Bell et al. 2017). Data were aggregated for the Santa Barbara Channel (including islands and mainland from Point Conception to Santa Monica Bay through Ventura County) or the San Diego region (mainland coast from the US-Mexico through Orange County including Santa Catalina and San Clemente Islands). We used the 3-month running mean of kelp canopy biomass during the period leading into the spawning season (September–November) because marked declines in reproductive capacity require several months of consistently low food supply (Okamoto 2014).

Adult sea urchin density in the Channel Islands (annual, 1997–2016, Santa Barbara Channel only)

The abundance of adult sea urchins can also fluctuate over time, which can affect larval production and supply. We used the spatial geometric mean of adult biomass density (kg m^{-2}) of purple sea urchins, calculated from surveys of density and size structure from the Channel Islands Kelp Forest Monitoring program (Kushner et al. 2013) and a size-biomass model from the Santa Barbara Coastal LTER (Reed 2018) as an index of the spawning biomass of purple sea urchins in the Santa Barbara Channel. We used the geometric mean (exponentiated log-scale mean) as it accounts for spatial differences in overall mean abundance among sites. We use a biomass index that incorporates size structure and density instead of just density because individual maximum fecundity increases with size. For details on calculation of biomass from the KFM data, see the Supporting Information.

We allowed regression coefficients to vary among major regions (Fort Bragg, Santa Barbara, and San Diego sites). We used this level of inference because the covariates are aggregated over spatial regions that encompass all sites within a region due to the long PLD of sea urchins. The regression analyses included either all global covariates (ENSO, PDO, NPGO) or all local covariates (temperature, chlorophyll, adult densities, giant kelp biomass, and the Bakun upwelling index). We conducted separate analyses for these two groups of

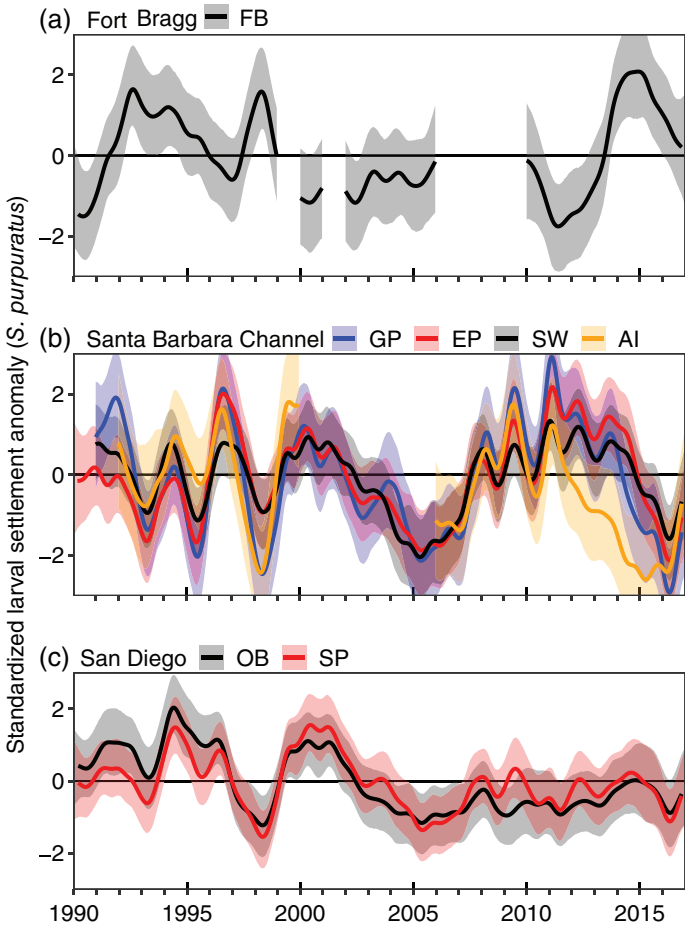

Fig. 3. Standardized annual scale trends (log-scale, standardized to one SD) of larval settlement *S. purpuratus* from 1990 through 2016 for: (**a**) Fort Bragg, (**b**) sites in the Santa Barbara Channel, and (**c**) sites in San Diego. Colors within represent individual sites associated with the legend. Interannual trends are estimated using a 3/2 Matérn Gaussian process covariance within a Bayesian multivariate state-space model accounting for spatiotemporal correlations.

covariates because global indices were directly correlated with local covariates, or in the case of temperature were partially derived from them. For the analysis with local covariates, we isolated data to 1997 and onward to accommodate the range of chlorophyll data availability, while global analysis included all data. Thus, our analyses provided nonmechanistic explanatory variables for global covariates and mechanistic explanatory variables for local covariates.

Results

Spatiotemporal trends in larval settlement

Substantial interannual variability in larval settlement of *S. purpuratus* was observed among years (Fig. 3, Supporting Information Fig. S1). Fluctuations in larval settlement were highly synchronous among sites within each of the two regions in the Southern California Bight (r = 0.73 and 0.85 for sites within the Santa Barbara Channel and San Diego, respectively; Fig. 3b,c). Within the Santa Barbara Channel, pairwise correlations in interannual trends involving Gaviota, Ellwood, and Stearns Wharf were higher (r = 0.86–0.90) than those involving Anacapa (r = 0.46–0.71). Anacapa began to decline in 2012, while the declines at the other sites did not begin until 2014 (Fig. 3b, Supporting Information Fig. S1b–e). While all of the Santa Barbara Channel sites except Anacapa exhibited eight continuous years of above average settlement following the low in 2005, San Diego sites remained mostly below average after 2003(Fig. 3c, Supporting Information Fig. S1f,g). This trend produced modest synchrony among San Diego and Santa Barbara sites from 1991 through 2007 (mean r = 0.68), but none thereafter (mean r = –0.06). In contrast, interannual trends in larval settlement at Fort Bragg were largely uncorrelated throughout the time series with sites in the Santa Barbara Channel (Fig. 3a vs. 3b, mean r = –0.23) and sites in San Diego (Fig. 3a vs. Fig. 3c; mean r = 0.12).

Larval settlement in southern California (San Diego and the Santa Barbara Channel) was highly seasonal, with similar patterns among sites (Fig. 4a, Supporting Information Fig. S2). On average, 90% of recruitment occurred from March to July with a single peak in late April/early May (Fig. 4a, Supporting Information Fig. S2), and by July settlement, on average, was an order of magnitude lower than during the April–May peak, and by September is two orders of magnitude lower. By contrast, recruitment at Fort Bragg in northern California extended over a longer period of time (90% occurred, between January and September) and typically included two peaks per year (a large peak around July and a smaller peak in February and March;

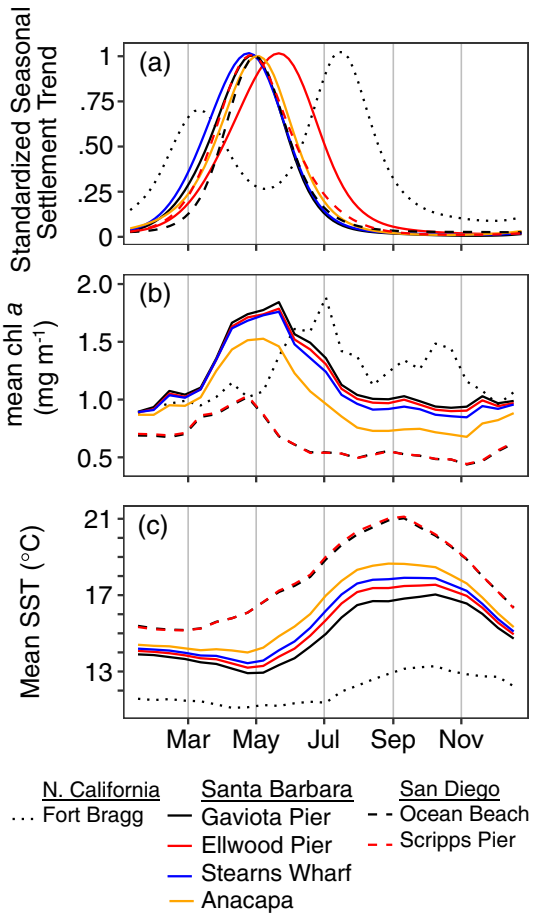

Fig. 4. Seasonal trends at each site for: (**a**) standardized larval settlement of *S. purpuratus*, (**b**) biweekly mean sea surface Chl *a*, and (**c**) biweekly mean SST. The seasonal trend in larval settlement at each site was standardized by the mean maximum seasonal value. Chl *a* and SST were measured using satellite imagery within 25 km of the coastline and 150 km alongshore of the location where settlement was sampled (hatched areas in Fig. 1). See "Methods" section for details. For site-specific and interannual variability in seasonal dynamics, see Supporting Information Fig. S3.

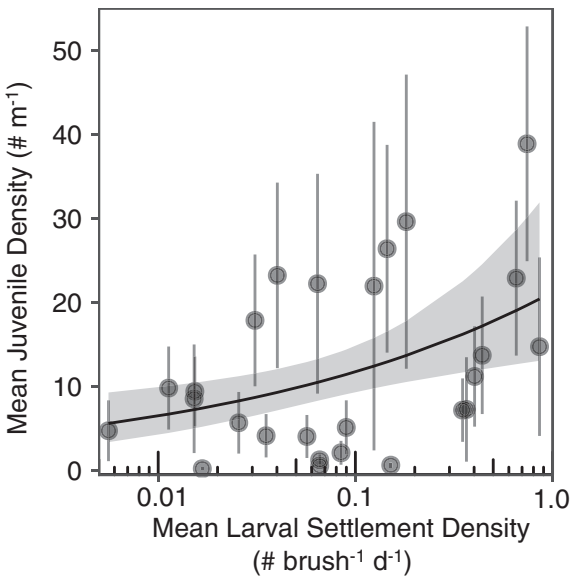

Fig. 5. The relationship between the summer density of juvenile purple sea urchins on reefs in the Santa Barbara Channel and the density of recruits on larval collectors during March–July of the previous year (i.e., 12–20 months prior). Points and error bars represent annual means (± SE) averaged over all sites. The line with the band represents the estimated relationship and 95% uncertainty interval.

Fig. 4a). The seasonal peaks in settlement in southern California coincided with peaks in sea surface chlorophyll (Fig. 4a vs. 4b) and troughs in SST (Fig. 4a vs. 4c). At Fort Bragg in northern California the primary peak occurred slightly after the peak in Chl *a* (Fig. 4a vs. 4b). These peaks in settlement were largely consistent among years, albeit with large variability in magnitude (shown by red lines in Supporting Information Fig. S1) and some interannual variability within sites (*see* Supporting Information Fig. S3 for a comparison in seasonal trend among years).

Relationship between benthic year-class strength and larval settlement

Recruitment of juvenile purple urchins at shallow subtidal reefs in the Santa Barbara Channel exhibited a significant, positive correlation with larval settlement to brushes 12–20 months prior (Fig. 5, negative binomial GLMM – $\chi^2_{df=1}$ = 9.48, p = 0.002). These results are robust to whether collection sites included only Anacapa (the sole site in the Channel Islands) or incorporated serial correlation using a site-specific first-order autoregressive model in the error covariance matrix. Years with the highest larval settlement corresponded with a nearly three-fold increase in the mean density of juvenile urchins two summers later (Fig. 5). Over the time series, average settlement densities in the Santa Barbara Channel varied by more than three orders of magnitude among years. This interannual variation in settlement (averaged across the sites in the Santa Barbara Channel) corresponded to more than a threefold increase in the density of benthic juveniles on average.

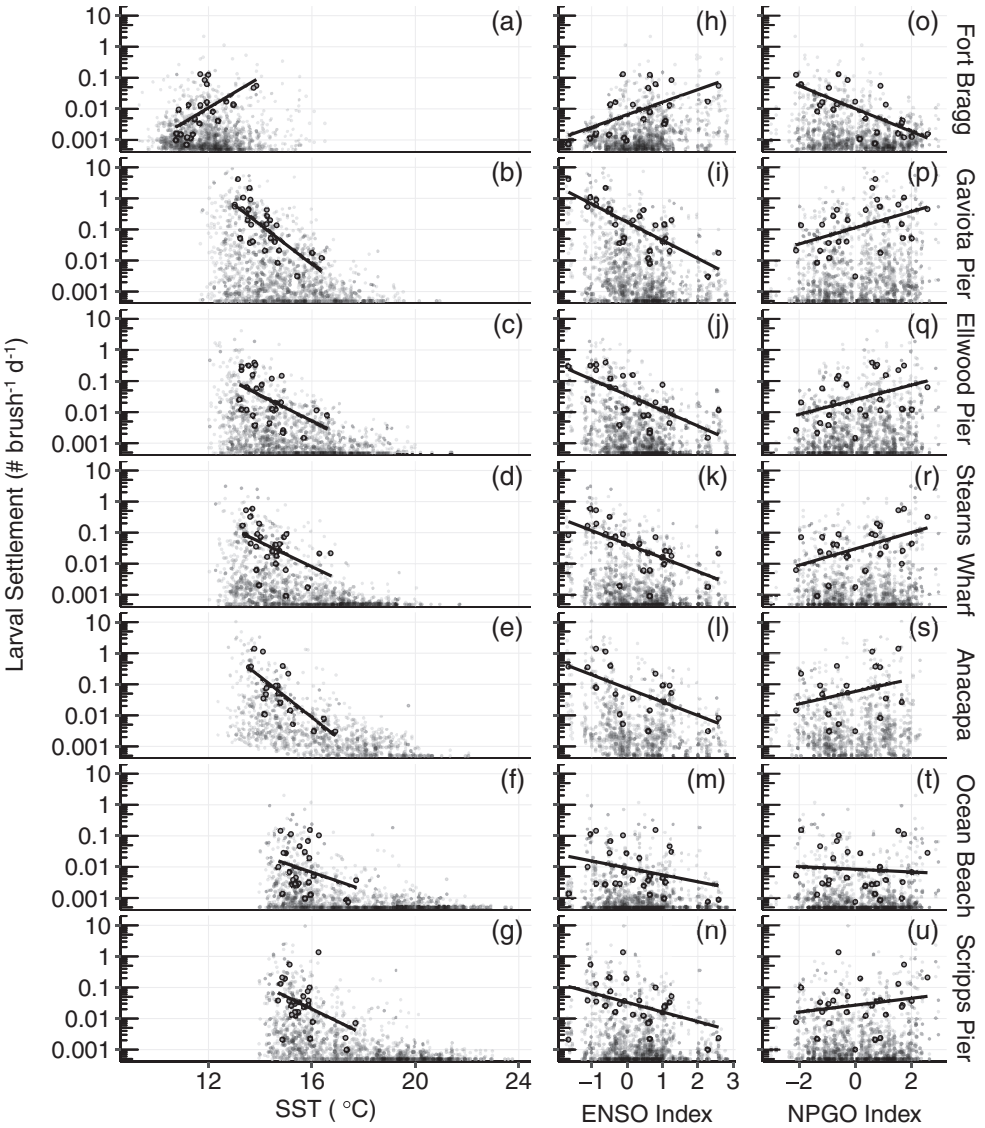

Fig. 6. The relationship between daily larval settlement of purple sea urchins and three climate variables: (**a**–**g**) SST, (**h**–**n**) the multivariate ENSO index, and (**o**–**u**) the NPGO. Small gray points represent biweekly means and black points and lines represent annual means.

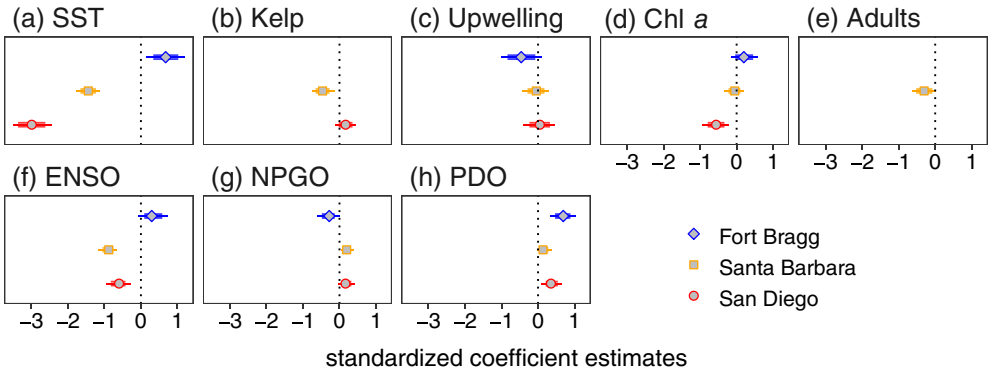

Fig. 7. Standardized Bayesian multiple regression coefficients for relationships between *S. purpuratus* settlement and local covariates (**a**–**e**) or global climatic indices (**f**–**h**). Models with global and local variables were fit separately. Coefficients were estimated using a multiple regression nested within a Bayesian multivariate time series model. Coefficients are a priori biased toward zero using a regularized horseshoe prior for variable selection. For details, see "Methods" section, Fig. 2, and Supporting Information for details.

Relationships between larval settlement and biotic and abiotic conditions

Larval settlement of purple urchins showed strong correlations with local SST (Figs. 6a–g, 7a) as well as the major climate indices (e.g., ENSO—Figs. 6h–n, 7f). For temperature and ENSO, the sign of the correlation at Fort Bragg was opposite that at sites in the Santa Barbara Channel and San Diego. The correlation between settlement and temperature varied from strongly negative at sites in San Diego and Santa Barbara to positive at the Fort Bragg site. Correlations between larval settlement and adult urchin density, upwelling, chlorophyll, and kelp biomass were either not different from zero or negative, which was opposite of that expected at all sites (Fig. 7b–e). Larval settlement and sea surface chlorophyll were uncorrelated at Fort Bragg and in the Santa Barbara Channel and negatively correlated in San Diego—the opposite of the hypothesized relationship that more food in the plankton would lead to higher larval settlement (Fig. 7d). The network of correlations among these variables is depicted in Supporting Information Fig. S3.

Larval settlement in southern California was orders of magnitude lower during warm, El Niño conditions and during the negative phase of the NPGO with the more southern sites in San Diego responding more strongly to temperature than those further north in the Santa Barbara Channel (Fig. 7a). In contrast, Fort Bragg, the northern most site, responded positively to warmer El Niño conditions, negatively to the NPGO, and positively to the PDO. Importantly, relationships observed between larval settlement and ENSO and temperature in southern California were opposite of those observed at Fort Bragg (Fig. 7f,g). The correlations between larval settlement and SST and ENSO occurred on roughly 3–5 yr cycles, while the correlation with NGPO and PDO occurred on decadal scales.

Discussion

Climate variability can significantly impact marine ecosystems by affecting recruitment, which in turn influences the dynamics of populations and communities. Yet determining which species and locations will respond to shifting climate remains a difficult task. Using a multidecadal, high frequency, and spatially extensive time series, we show how large-scale climatic variation can give rise to spatially different responses in the settlement of larval sea urchins. We found that settlement patterns were synchronous within Santa Barbara and San Diego and synchronous between these two regions until the late 2000s. Importantly, these sites responded negatively to elevated temperature and ENSO events. This contrasted sharply with settlement at our northern California site (Fort Bragg), which was positively correlated to temperature and ENSO. This difference was most obvious during the two strongest ENSO events in 1998 and 2014, when settlement responded dramatically in opposite directions.

While many recruitment-environment correlations often break down over time (Myers 1998), the correlations between oceanographic factors and larval settlement in our study were evident over a 27-yr period that included multiple major ENSO events and several minor ones. We observed repeatable patterns of diminished larval settlement in response to temperature and ENSO events in southern California with opposite responses at Fort Bragg in northern California. Others have found larval settlement in sea urchins to be positively or negatively related to temperature depending on the species (Ebert 1983; Himmelman 1986; Hernández et al. 2010). Our study is among the first to show that the relationship between larval settlement and temperature can vary dramatically within a species depending on location. Although sea urchin larval settlement data at the fine temporal scale of our study are not available prior to 1990, there is a history of evidence for ENSO-related recruitment failures in sea urchin populations of southern California. Between 1969 and the early 1980s, recruitment of juvenile sea urchins was anomalously low during El Niño years (Ebert 1983; Tegner and Dayton 1991). How patterns of larval settlement change in the future will undoubtedly depend on the processes underlying their associations with ENSO events.

Climate-related fluctuations in the supply of larvae have been hypothesized to affect coastal species around the world (Underwood and Fairweather 1989; Grosberg and Levitan 1992; Caley et al. 1996). In the case of sea urchins, larval supply has been implicated for dramatic changes in the state of benthic communities (Estes and Duggins 1995; Ling et al. 2009; Hernández et al. 2010). Yet empirically demonstrating such links has historically proved challenging because recruitment can be attenuated by high mortality of newly settled larvae (Connell 1985; Rowley 1989), increasing the need for high frequency data of larval settlement spanning multiple years. Data such as ours that meet these criteria are rare.

The potential factors affecting larval supply that we examined other than temperature and climate showed no meaningful correlations with larval settlement. Of particular note was the lack of a correlation with ocean chlorophyll revealed by our analyses. This finding differed from that observed for the tropical sea urchin *Diadema aff. antillarum* (Hernández et al. 2010) and other echinoderms (e.g., Lamare and Barker 1999; Fabricius et al. 2010) and highlights a need for exploring mechanistically how spatial and temporal variability in ocean circulation and phytoplankton productivity affect patterns of larval settlement. These outcomes do not suggest that food is not important for urchin larvae, only that interannual variation therein did not explain the interannual trends in settlement. Indeed, the mean seasonal trends in both southern and northern California (which we show are synchronous in southern California) corresponded to peaks in primary productivity, and both are regions of high productivity (Kahru et al. 2012).

Similar to other studies (Shanks and Shearman 2009; Shanks and Morgan 2018), we found no relationship between large-scale fluctuations in indices of upwelling and larval settlement, which runs counter to hypotheses that large-scale coastal upwelling shapes patterns of larval supply by broadly altering productivity and retention (Roughgarden et al. 1991; Menge and Menge 2013). The major ocean currents in our study system (the Southern California Counter Current and the California Current) are characterized by stochastic and spatially variable eddies, fronts, filaments, and bores (e.g., DiGiacomo and Holt 2001; Bassin et al. 2005; Davis et al. 2008), whereas flows closer to shore tend to promote larval retention along wave exposed shores (Morgan et al. 2016; Shanks et al. 2017). As a result, offshore transport and retention off the coast of California is spatially nuanced and temporally inconsistent (Shanks and Eckert 2005). Such heterogeneity not only influences larval transport, but also when and where larvae encounter productive food environments. Consequently, if larval food limitation plays a role in shaping the dynamics of urchin settlement at our sites, then it likely arises out of more complex dynamics than our spatially aggregated composite metrics were able to detect. For example, processes that shape stratification, front formation, and spatially isolated phytoplankton blooms in combination with larval behavior may play a more important role than predicted by simplifications of the higher or lower spatially averaged phytoplankton biomass or greater or lesser coastal upwelling.

The oceanographic processes that affect spatial distribution and survival of larvae may also affect predation driven mortality by altering the densities of predators and their larval prey. While predation on echinoplutei certainly occurs, its relative importance in shaping larval supply to the benthos remains difficult to quantify (Rumrill 1990; Vaughn and Allen 2010). For *S. purpuratus* plutei, predation may be lower than for other taxa because they contain chemical and structural defenses and display predator avoidance behavior (Cowden et al. 1984), particularly at later stages of development, which are far less susceptible to predation (Rumrill 1985). This is supported by field studies that have shown predator mortality to be comparatively low for echinoids (Johnson and Shanks 2003; Allen and McAlister 2007), which in part may be due to the fact that accounting for natural densities of echinoplutei can dramatically reduce estimates of laboratory predation rates (Johnson and Shanks 1997). Integrating mechanistic models of ocean circulation and mortality was beyond the scope of our study, yet such approaches are needed to develop a more thorough understanding of processes that control settlement dynamics across large gradients in oceanographic settings as they can control both population dynamics and range limits (Gaylord and Gaines 2000).

Although climate-related changes can alter larval supply via their effects on the production of larvae by adults, we found no relationship between larval settlement and regional adult abundance or adult food (kelp). While fisheries research relies heavily on stock-recruit dynamics, there is continual debate about whether adult dynamics actually control recruitment patterns (Gilbert 1997; Szuwalski et al. 2015). The lack of a positive correlation between adults and larval settlement that we found for purple sea urchins adds to this debate by showing that high abundances of adult urchins and kelp averaged across large spatial scales did not translate into high larval settlement. We note that spatial structure in the dynamics of kelp and adult urchins may have affected this outcome. For example, modest but uniform densities of adult sea urchins in food rich kelp forests can provide very different outcomes for the production of embryos compared to mosaics of dense adults in barren patches interspersed with forested patches having few adults (Okamoto 2014). Indeed, previous work has demonstrated that assessing population productivity in spatially structured populations requires a spatially structured analysis to account for processes of population regulation and competition (Chesson 1996, 1998; Chesson et al. 2005; Thorson et al. 2015). That said, we found no evidence that synchronous fluctuations in settlement arose from broad-scale collapses and proliferations in populations of adult sea urchins or kelp at the appropriate lags and time-scales.

Temperature-related effects on larval production and survival and ENSO-related changes in currents or oceanographic

features that transport larvae represent two possible explanations for the spatially opposing correlations between larval settlement and temperature and ENSO that we observed. Many species have upper temperature thresholds beyond which reproduction is impaired that are well below the lethal limits for adults. Temperatures in southern California kelp forests routinely exceed 17°C during ENSO events (Reed et al. 2016), which may adversely affect larval supply of purple sea urchins by limiting gamete production (Cochran and Engelmann 1975; Basch and Tegner 2007), fertilization (Schroeder and Battaglia 1985), larval development and gene expression (Runcie et al. 2012; Padilla-Gamiño et al. 2013; Wong et al. 2018), and larval survival (Azad et al. 2012). Such effects may in part explain why larval settlement at Fort Bragg, where SSTs rarely exceed 16°C was not negatively correlated with temperature. Unfortunately, there are no long-term data sets on reproductive activity or planktonic larval densities and distributions to evaluate if and how the interannual and seasonal trends observed here correspond to variation in reproductive activity and transport of larvae.

Regional circulation is considered to be an important driver of larval supply for many species, including those in the Southern California Bight (Hereu et al. 2004; Broitman et al. 2005; Blanchette et al. 2006; McManus and Woodson 2012; Woodson et al. 2012). ENSO events can cause major changes in patterns of ocean circulation in the Southern California Bight and elsewhere along the US west coast (Lynn and Bograd 2002; Mitarai et al. 2009; Pineda and Reyns 2017). Spatial variability in such patterns could explain the opposing climatic responses in larval settlement between Fort Bragg and our sites in southern California. El Niño events in southern California are associated with lower stratification and reduced internal waves that promote the onshore transport of larvae (Shanks 1983; Pineda 1994; Pineda et al. 2018). In contrast, El Nino events in northern California are often associated with relaxed upwelling, downwelling Kelvin waves, and increased stratification (Chavez et al. 2002). Although we cannot definitively partition out the effects of climate associated changes in temperature and circulation on recruitment, our observations of larval settlement and subsequent year-class strength point strongly to broader-scale ocean climate effects.

Our finding that larval settlement was a good predictor of regional year class strength in natural populations indicates that large fluctuations in larval settlement of this prominent herbivore could have far-reaching ecological impacts that resonate throughout marine ecosystems across a broad geographic region (Pearse 2006). For example, the high settlement that we observed at Fort Bragg in 2013–2015 coupled with a period of anomalously warm water may explain the marked increase in the abundance of purple urchins and coincident loss of canopy forming kelps reported for northern California beginning in 2014 (Rogers-Bennett and Catton 2019). Although regional processes appear to drive broad-scale patterns of larval settlement in sea urchins, local hydrodynamics and other factors contribute to considerable fine-scale spatial variation in larval supply and settlement in sea urchins (Ebert et al. 1994; Schroeter et al. 1996, 2009; Hereu et al. 2004; Farina et al. 2018). For example, pelagic larval abundance and settlement of *Paracentrotus lividus* varies substantially in space (Hereu et al. 2004; Prado et al. 2012) as does post-settlement survival and abundance due to localized and habitat-dependent effects (Prado et al. 2012; Boada et al. 2018). Our inferences focused on temporal trends and comparison of regional-scale patterns, rather than trying to infer causes and consequences of variation in average settlement in space. Despite these caveats, our analyses show remarkable synchrony in settlement within southern California and strong association with regional benthic recruitment in the Santa Barbara Channel. Collectively, our results suggest that predicted changes in ocean climate that lead to more frequent or severe marine heat waves (Frölicher and Laufkötter 2018) will reduce purple urchin recruitment in southern California, but increase it in northern California with potentially cascading effects on benthic ecosystems similar to those recently observed in northern California.

Oceans are experiencing simultaneous shifts in temperature, water chemistry, productivity, and circulation, which have profound consequences for the ecological structure and function of marine systems and the services that they provide (Wong et al. 2014). Our findings provide valuable insights into the ecological consequences of climate-related effects on patterns of larval settlement of an important reef herbivore whose distribution spans most of the Pacific coast of North America. Future investigations aimed at determining the specific biotic and abiotic processes that regulate larval settlement in ecological important species such as *S. purpuratus* will undoubtedly improve our understanding of how climate fluctuations affect regional population dynamics to alter the structure and functions of marine ecosystems.

References

Allen, J. D., and J. S. McAlister. 2007. Testing rates of planktonic versus benthic predation in the field. J. Exp. Mar. Biol. Ecol. **347**: 77–87. doi:10.1016/j.jembe.2007.03.010

Andrew, N., and others. 2003. Status and management of world sea urchin fisheries. Oceanogr. Mar. Biol. **40**: 343–425.

Azad, A. K., C. M. Pearce, and R. S. McKinley. 2012. Influence of stocking density and temperature on early development and survival of the purple sea urchin, *Strongylocentrotus purpuratus* (Stimpson, 1857). Aquacult. Res. **43**: 1577–1591. doi:10.1111/j.1365-2109.2011.02960.x

Bakun, A. 1973. Coastal upwelling indices, west coast of North America 1945-71. NOAA Technical Report, NMFS SSRF-671, p. 96.

Basch, L. V., and M. J. Tegner. 2007. Reproductive responses of purple sea urchin (*Strongylocentrotus purpuratus*) populations to environmental conditions across a coastal depth gradient. Bull. Mar. Sci. **81**: 255–282.

Bassin, C. J., L. Washburn, M. Brzezinski, and E. McPhee-Shaw. 2005. Sub-mesoscale coastal eddies observed by high frequency radar: A new mechanism for delivering nutrients to kelp forests in the Southern California Bight. Geophys. Res. Lett. **32**, L12604. doi:10.1029/2005GL023017

Bell, T., K. Cavanaugh, and D. Siegel. 2017. SBC LTER: Time series of quarterly NetCDF files of kelp biomass in the canopy from Landsat 5, 7 and 8, 1984–2016 (ongoing) ver 10. Environmental Data Initiative. doi:10.6073/pasta/817d2c24ebd78621869e17d94ba0df0c.

Bell, T. W., K. C. Cavanaugh, D. C. Reed, and D. A. Siegel. 2015. Geographical variability in the controls of giant kelp biomass dynamics. J. Biogeogr. **42**: 2010–2021. doi:10.1111/jbi.12550

Bertram, D. F., and R. R. Strathmann. 1998. Effects of maternal and larval nutrition on growth and form of planktotrophic larvae. Ecology **79**: 315–327. doi:10.1890/0012-9658(1998)079[0315:EOMALN]2.0.CO;2

Blanchette, C. A., B. R. Broitman, and S. D. Gaines. 2006. Intertidal community structure and oceanographic patterns around Santa Cruz Island, CA, USA. Mar. Biol. **149**: 689–701. doi:10.1007/s00227-005-0239-3

Boada, J., S. Farina, R. Arthur, J. Romero, P. Prado, and T. Alcoverro. 2018. Herbivore control in connected seascapes: Habitat determines when population regulation occurs in the life history of a key herbivore. Oikos **127**: 1195–1204. doi:10.1111/oik.05060

Broitman, B. R., C. A. Blanchette, and S. D. Gaines. 2005. Recruitment of intertidal invertebrates and oceanographic variability at Santa Cruz Island, California. Limnol. Oceanogr. **50**: 1473–1479. doi:10.4319/lo.2005.50.5.1473

Burt, J. M., M. T. Tinker, D. K. Okamoto, K. W. Demes, K. Holmes, and A. K. Salomon. 2018. Sudden collapse of a mesopredator reveals its complementary role in mediating rocky reef regime shifts. Proc. R. Soc. B Biol. Sci. **285**. doi:10.1098/rspb.2018.0553

Byrne, M., M. Ho, P. Selvakumaraswamy, H. D. Nguyen, S. A. Dworjanyn, and A. R. Davis. 2009. Temperature, but not pH, compromises sea urchin fertilization and early development under near-future climate change scenarios. Proc. R. Soc. B Biol. Sci. **276**: 1883–1888. doi:10.1098/rspb.2008.1935

Cai, W., and others. 2014. Increasing frequency of extreme El Niño events due to greenhouse warming. Nat. Clim. Chang. **4**: 111–116. doi:10.1038/nclimate2100

Caley, M., M. Carr, M. Hixon, T. Hughes, G. Jones, and B. Menge. 1996. Recruitment and the local dynamics of open marine populations. Annu. Rev. Ecol. Syst. **27**: 477–500. doi:10.1146/annurev.ecolsys.27.1.477

Carpenter, B., and others. 2016. Stan: A probabilistic programming language. J. Stat. Softw. **76**: 1–32. doi:10.18637/jss.v076.i01

Carvalho, C. M., N. G. Polson, and J. G. Scott. 2010. The horseshoe estimator for sparse signals. Biometrika **97**: 465–480. doi:10.1093/biomet/asq017

Chavez, F., and others. 2002. Biological and chemical consequences of the 1997–1998 El Niño in central California waters. Prog. Oceanogr. **54**: 205–232. doi:10.1016/S0079-6611(02)00050-2

Chesson, P. 1996. Matters of scale in the dynamics of populations and communities, p. 353–368. *In* R. Floyd, A. Sheppard, and P. de Barro [eds.], Frontiers of population ecology. CSIRO.

Chesson, P. 1998. Spatial scales in the study of reef fishes: A theoretical perspective. Aust. J. Ecol. **23**: 209–215. doi:10.1111/j.1442-9993.1998.tb00722.x

Chesson, P., M. J. Donahue, B. A. Melbourne, and A. L. Sears. 2005. Scale transition theory for understanding mechanisms in metacommunities, p. 279–306. *In* M. Holyoak, M. Leibold, and R. Holt [eds.], Metacommunities: Spatial dynamics and ecological communities. Univ. of Chicago Press.

Cochran, R. C., and F. Engelmann. 1975. Environmental regulation of the annual reproductive season of *Strongylocentrotus purpuratus* (Stimpson). Biol. Bull. **148**: 393–401. doi:10.2307/1540516

Connell, J. H. 1985. The consequences of variation in initial settlement vs. post-settlement mortality in rocky intertidal communities. J. Exp. Mar. Biol. Ecol. **93**: 11–45. doi:10.1016/0022-0981(85)90146-7

Cowden, C., C. M. Young, and F. Chia. 1984. Differential predation on marine invertebrate larvae by two benthic predators. Mar. Ecol. Prog. Ser. **14**: 145–149. doi:10.3354/meps014145

Davis, R. E., M. D. Ohman, D. L. Rudnick, and J. T. Sherman. 2008. Glider surveillance of physics and biology in the southern California Current System. Limnol. Oceanogr. **53**: 2151–2168. doi:10.4319/lo.2008.53.5_part_2.2151

Di Lorenzo, E., and others. 2008. North Pacific Gyre Oscillation links ocean climate and ecosystem change. Geophys. Res. Lett. **35**, L08607. doi:10.1029/2007GL032838

Di Lorenzo, E., and others. 2013. Synthesis of Pacific Ocean climate and ecosystem dynamics. Oceanography **26**: 68–81. doi:10.5670/oceanog.2013.76

DiGiacomo, P. M., and B. Holt. 2001. Satellite observations of small coastal ocean eddies in the Southern California Bight. J. Geophys. Res. Oceans **106**: 22521–22543. doi:10.1029/2000JC000728

Ebert, T. A. 1983. Recruitment in echinoderms. Echinoderm Stud. **1**: 169–203.

Ebert, T. A. 2010. Demographic patterns of the purple sea urchin *Strongylocentrotus purpuratus* along a latitudinal gradient, 1985-1987. Mar. Ecol. Prog. Ser. **406**: 105–120. doi:10.3354/meps08547

Ebert, T. A., S. Schroeter, J. Dixon, and P. Kalvass. 1994. Settlement patterns of red and purple sea urchins (*Strongylocentrotus franciscanus* and *S. purpuratus*) in California, USA. Mar. Ecol. Prog. Ser. **111**: 41–52. doi:10.3354/meps111041

Edmunds, P. J., and R. C. Carpenter. 2001. Recovery of *Diadema antillarum* reduces macroalgal cover and increases abundance of juvenile corals on a Caribbean reef. Proc. Natl. Acad. Sci. USA **98**: 5067–5071. doi:10.1073/pnas.071524598

Estes, J. A., and D. O. Duggins. 1995. Sea otters and kelp forests in Alaska: Generality and variation in a community ecological paradigm. Ecol. Monogr. **65**: 75–100. doi:10.2307/2937159

Fabricius, K., K. Okaji, and G. De'Ath. 2010. Three lines of evidence to link outbreaks of the crown-of-thorns seastar *Acanthaster planci* to the release of larval food limitation. Coral Reefs **29**: 593–605. doi:10.1007/s00338-010-0628-z

Farina, S., G. Quattrocchi, I. Guala, and A. Cucco. 2018. Hydrodynamic patterns favouring sea urchin recruitment in coastal areas: A Mediterranean study case. Mar. Environ. Res. **139**: 182–192. doi:10.1016/j.marenvres.2018.05.013

Feehan, C. J., and R. E. Scheibling. 2014. Effects of sea urchin disease on coastal marine ecosystems. Mar. Biol. **161**: 1467–1485. doi:10.1007/s00227-014-2452-4

Field, C. M., and C. Walker. 2003. A site profile of the Kachemak Bay Research Reserve, a unit of the National Estuarine Research Reserve System. Kachemak Bay Research Reserve.

Filbee-Dexter, K., and R. E. Scheibling. 2014. Sea urchin barrens as alternative stable states of collapsed kelp ecosystems. Mar. Ecol. Prog. Ser. **495**: 1–25. doi:10.3354/meps10573

Fisher, J. L., W. T. Peterson, and S. G. Morgan. 2014. Does larval advection explain latitudinal differences in recruitment across upwelling regimes? Mar. Ecol. Prog. Ser. **503**: 123–137. doi:10.3354/meps10732

Foster, M. C., J. E. Byrnes, and D. C. Reed. 2015. Effects of five southern California macroalgal diets on consumption, growth, and gonad weight, in the purple sea urchin *Strongylocentrotus purpuratus*. PeerJ **3**: e719. doi:10.7717/peerj.719

Frölicher, T. L., and C. Laufkötter. 2018. Emerging risks from marine heat waves. Nature communications **9**: 650. doi:10.1038/s41467-018-03163-6

Gaylord, B., and S. D. Gaines. 2000. Temperature or transport? Range limits in marine species mediated solely by flow. Am. Nat. **155**: 769–789. doi:10.1086/303357

Gilbert, D. 1997. Towards a new recruitment paradigm for fish stocks. Can. J. Fish. Aquat. Sci. **54**: 969–977. doi:10.1139/f96-272

Gonor, J. J. 1973. Reproductive cycles in Oregon populations of the echlnoid, *Strongylocentrotus purpuratus* (Stimpson). I. Annual gonad growth and ovarian gametogenic cycles. J. Exp. Mar. Biol. Ecol. **12**: 45–64. doi:10.1016/0022-0981(73)90037-3

Grosberg, R. K., and D. R. Levitan. 1992. For adults only? Supply-side ecology and the history of larval biology. Trends Ecol. Evol. **7**: 130–133. doi:10.1016/0169-5347(92)90148-5

Hereu, B., M. Zabala, C. Linares, and E. Sala. 2004. Temporal and spatial variability in settlement of the sea urchin *Paracentrotus lividus* in the NW Mediterranean. Mar. Biol. **144**: 1011–1018. doi:10.1007/s00227-003-1266-6

Hernández, J. C., S. Clemente, D. Girard, Á. Pérez-Ruzafa, and A. Brito. 2010. Effect of temperature on settlement and postsettlement survival in a barrens-forming sea urchin. Mar. Ecol. Prog. Ser. **413**: 69–80. doi:10.3354/meps08684

Himmelman, J. H. 1986. Population biology of green sea urchins on rocky barrens. Mar. Ecol. Prog. Ser. **33**: 295–306. doi:10.3354/meps033295

Hoegh-Guldberg, O., and J. S. Pearse. 1995. Temperature, food availability, and the development of marine invertebrate larvae. Am. Zool. **35**: 415–425. doi:10.1093/icb/35.4.415

Johnson, K. B., and A. L. Shanks. 1997. The importance of prey densities and background plankton in studies of predation on invertebrate larvae. Mar. Ecol. Prog. Ser. **158**: 293–296. doi:10.3354/meps158293

Johnson, K. B., and A. L. Shanks. 2003. Low rates of predation on planktonic marine invertebrate larvae. Mar. Ecol. Prog. Ser. **248**: 125–139. doi:10.3354/meps248125

Kahru, M., R. M. Kudela, M. Manzano-Sarabia, and B. G. Mitchell. 2012. Trends in the surface chlorophyll of the California Current: Merging data from multiple ocean color satellites. Deep-Sea Res. Part II Top. Stud. Oceanogr. **77**: 89–98. doi:10.1016/j.dsr2.2012.04.007

Kato, S., and S. C. Schroeter. 1985. Biology of the red sea urchin, *Strongylocentrotus franciscanus*, and its fishery in California. Mar. Fish. Rev. **47**: 1–20.

Kushner, D. J., A. Rassweiler, J. P. McLaughlin, and K. D. Lafferty. 2013. A multi-decade time series of kelp forest community structure at the California Channel Islands: Ecological Archives E094-245. Ecology **94**: 2655–2655. doi:10.1890/13-0562R.1

Lafferty, K. D. 2004. Fishing for lobsters indirectly increases epidemics in sea urchins. Ecol. Appl. **14**: 1566–1573. doi:10.1890/03-5088

Lamare, M. D., and M. F. Barker. 1999. In situ estimates of larval development and mortality in the New Zealand sea urchin *Evechinus chloroticus* (Echinodermata: Echinoidea). Mar. Ecol. Prog. Ser. **180**: 197–211. doi:10.3354/meps180197

Lewandowski, D., D. Kurowicka, and H. Joe. 2009. Generating random correlation matrices based on vines and extended onion method. Journal of multivariate analysis **100**: 1989–2001. doi:10.1016/j.jmva.2009.04.008

Ling, S., C. Johnson, K. Ridgway, A. Hobday, and M. Haddon. 2009. Climate-driven range extension of a sea urchin: Inferring future trends by analysis of recent population dynamics. Glob. Chang. Biol. **15**: 719–731. doi:10.1111/j.1365-2486.2008.01734.x

Lynn, R., and S. Bograd. 2002. Dynamic evolution of the 1997–1999 El Niño–La Niña cycle in the southern California Current System. Prog. Oceanogr. **54**: 59–75. doi:10.1016/S0079-6611(02)00043-5

Magnusson, A., and others. 2017. glmmTMB: Generalized linear mixed models using template model builder (version R

package version 0.1.3). Available from https://github.com/glmmTMB. Accepted 19 November 2019.

Mantua, N. J., S. R. Hare, Y. Zhang, J. M. Wallace, and R. C. Francis. 1997. A Pacific interdecadal climate oscillation with impacts on salmon production. Bull. Am. Meteorol. Soc. **78**: 1069–1080. doi:10.1175/1520-0477(1997)078<1069:APICOW>2.0.CO;2

Mantua, N. J., and S. R. Hare. 2002. The Pacific decadal oscillation. J. Oceanogr. **58**: 35–44. doi:10.1023/A:1015820616384

McManus, M. A., and C. B. Woodson. 2012. Plankton distribution and ocean dispersal. J. Exp. Biol. **215**: 1008–1016. doi:10.1242/jeb.059014

Menge, B. A., T. C. Gouhier, T. Freidenburg, and J. Lubchenco. 2011. Linking long-term, large-scale climatic and environmental variability to patterns of marine invertebrate recruitment: Toward explaining "unexplained" variation. J. Exp. Mar. Biol. Ecol. **400**: 236–249. doi:10.1016/j.jembe.2011.02.003

Menge, B. A., and D. N. Menge. 2013. Dynamics of coastal meta-ecosystems: The intermittent upwelling hypothesis and a test in rocky intertidal regions. Ecol. Monogr. **83**: 283–310. doi:10.1890/12-1706.1

Mitarai, S., D. Siegel, J. Watson, C. Dong, and J. McWilliams. 2009. Quantifying connectivity in the coastal ocean with application to the Southern California Bight. J. Geophys. Res. **114**: C10026. doi:10.1029/2008JC005166

Morgan, S. G. 2014. Behaviorally mediated larval transport in upwelling systems. Adv. Oceanogr. **2014**: 1–17. doi:10.1155/2014/364214

Morgan, S. G., J. L. Fisher, S. H. Miller, S. T. McAfee, and J. L. Largier. 2009. Nearshore larval retention in a region of strong upwelling and recruitment limitation. Ecology **90**: 3489–3502. doi:10.1890/08-1550.1

Morgan, S. G., A. L. Shanks, A. G. Fujimura, A. J. Reniers, J. MacMahan, C. D. Griesemer, M. Jarvis, and J. Brown. 2016. Surfzone hydrodynamics as a key determinant of spatial variation in rocky intertidal communities. Proc. R. Soc. B Biol. Sci. **283**: 20161017. doi:10.1098/rspb.2016.1017

Morgan, S. G. M., S. H. Miller, M. J. Robart, and J. L. Largier. 2018. Nearshore larval retention and cross-shelf migration of benthic crustaceans at an upwelling center. Front. Mar. Sci. **5**: 161.

Myers, R. A. 1998. When do environment–recruitment correlations work? Rev. Fish Biol. Fish. **8**: 285–305. doi:10.1023/A:1008828730759

Okamoto, D. K. 2014. The role of fluctuating food supply on recruitment, survival and population dynamics in the sea. Univ. of California Santa Barbara.

Olivares-Bañuelos, N. C., L. M. Enríquez-Paredes, L. B. Ladah, and J. De La Rosa-Vélez. 2008. Population structure of purple sea urchin *Strongylocentrotus purpuratus* along the Baja California peninsula. Fish. Sci. **74**: 804–812. doi:10.1111/j.1444-2906.2008.01592.x

Padilla-Gamiño, J. L., M. W. Kelly, T. G. Evans, and G. E. Hofmann. 2013. Temperature and CO_2 additively regulate physiology, morphology and genomic responses of larval sea urchins, *Strongylocentrotus purpuratus*. Proc. R. Soc. B Biol. Sci. **280**: 1–9. doi:10.1098/rspb.2013.0155

Pearse, J. S. 2006. Ecological role of purple sea urchins. Science **314**: 940–941. doi:10.1126/science.1131888

Pearse, J. S., V. B. Pearse, and K. K. Davis. 1986. Photoperiodic regulation of gametogenesis and growth in the sea urchin *Strongylocentrotus purpuratus*. J. Exp. Zool. **237**: 107–118. doi:10.1002/jez.1402370115

Piironen, J., and A. Vehtari. 2017. Sparsity information and regularization in the horseshoe and other shrinkage priors. Electron. J. Stat. **11**: 5018–5051. doi:10.1214/17-EJS1337SI

Pineda, J. 1994. Internal tidal bores in the nearshore: Warm-water fronts, seaward gravity currents and the onshore transport of neustonic larvae. J. Mar. Res. **52**: 427–458. doi:10.1357/0022240943077046

Pineda, J., and N. Reyns. 2017. Larval transport in the coastal zone: Biological and physical processes. *In* T. Carrier, A. Heyland, and A. Reitzel [eds.], Evolutionary ecology of marine invertebrate larvae. Oxford Univ. Press Evolutionary ecology of marine invertebrate larvae, p. 145–163.

Pineda, J., N. Reyns, and S. J. Lentz. 2018. Reduced barnacle larval abundance and settlement in response to large-scale oceanic disturbances: Temporal patterns, nearshore thermal stratification, and potential mechanisms. Limnol. Oceanogr. **63**: 2618–2629. doi:10.1002/lno.10964

Polson, N. G., and J. G. Scott. 2012. On the half-Cauchy prior for a global scale parameter. Bayesian Analysis **7**: 887–902. doi:10.1214/12-BA730

Prado, P., F. Tomas, S. Pinna, S. Farina, G. Roca, G. Ceccherelli, J. Romero, and T. Alcoverro. 2012. Habitat and scale shape the demographic fate of the keystone sea urchin *Paracentrotus lividus* in Mediterranean macrophyte communities. PLoS One **7**: e35170. doi:10.1371/annotation/7e978cb1-df3b-42f1-94d9-fcc424cf7167

Rasmussen C. E., Williams C. K. I. 2006 Gaussian Processes for Machine Learning. Cambridge, Massachusetts, The MIT Press.

Reed, D., L. Washburn, A. Rassweiler, R. Miller, T. Bell, and S. Harrer. 2016. Extreme warming challenges sentinel status of kelp forests as indicators of climate change. Nature Communications, **7**: 13757. doi:10.1038/ncomms13757

Reed, D. 2018. SBC LTER: Reef: Annual time series of biomass for kelp forest species, ongoing since 2000. doi:10.1063/1.468314

Reynolds, R. W., T. M. Smith, C. Liu, D. B. Chelton, K. S. Casey, and M. G. Schlax. 2007. Daily high-resolution-blended analyses for sea surface temperature. J. Clim. **20**: 5473–5496. doi:10.1175/2007JCLI1824.1

Rogers-Bennett, L., and C. Catton. 2019. Marine heat wave and multiple stressors tip bull kelp forest to sea urchin barrens. Sci. Rep. **9**: 1–9.

Rogers-Bennett, L., and D. K. Okamoto. 2020. *Mesocentrotus franciscanus* and *Strongylocentrotus purpuratus*, p. 593–608. *In* J. M. Lawrence [ed.], Sea urchins: Biology & ecology, v. **43**, 4th ed. Elsevier.

Roughgarden, J., S. Gaines, and H. Possingham. 1988. Recruitment dynamics in complex life cycles. Proc. Natl. Acad. Sci. USA **85**: 1460–1466.

Roughgarden, J., J. Pennington, D. Stoner, S. Alexander, and K. Miller. 1991. Collisions of upwelling fronts with the intertidal zone: The cause of recruitment pulses in barnacle populations of central California. Acta Oecol. **12**: 35–51.

Rowley, R. 1989. Settlement and recruitment of sea urchins (*Strongylocentrotus* spp.) in a sea-urchin barren ground and a kelp bed: Are populations regulated by settlement or post-settlement processes? Mar. Biol. **100**: 485–494. doi:10.1007/BF00394825

Rumrill, S. S. 1985. Differential mortality during the embryonic and larval lives. Echinodermata **24**: 333.

Rumrill, S. S. 1990. Natural mortality of marine invertebrate larvae. Ophelia **32**: 163–198. doi:10.1080/00785236.1990.10422030

Runcie, D. E., D. A. Garfield, C. C. Babbitt, J. A. Wygoda, S. Mukherjee, and G. A. Wray. 2012. Genetics of gene expression responses to temperature stress in a sea urchin gene network. Mol. Ecol. **21**: 4547–4562. doi:10.1111/j.1365-294X.2012.05717.x

Sathyendranath, S., and others. 2018. ESA ocean colour climate change initiative (Ocean_Colour_cci): Version 3.1 data. doi:10.5285/9c334fbe6d424a708cf3c4cf0c6a53f5

Schroeder, T., and D. Battaglia. 1985. "Spiral asters" and cytoplasmic rotation in sea urchin eggs: Induction in *Strongylocentrotus purpuratus* eggs by elevated temperature. J. Cell Biol. **100**: 1056–1062. doi:10.1083/jcb.100.4.1056

Schroeter, S., J. Dixon, T. Ebert, and J. Rankin. 1996. Effects of kelp forests *Macrocystis pyrifera* on the larval distribution and settlement of red and purple sea urchins *Strongylocentrotus franciscanus* and *S. purpuratus*. Mar. Ecol. Prog. Ser. **133**: 125–134. doi:10.3354/meps133125

Schroeter, S. C., H. M. Page, J. E. Dugan, C. S. Culver, B. Steele, R. Gutierrez, J. B. Richards, and D. Kushner. 2009. Scales of variability in larval settlement within the Channel Islands National Marine Sanctuary and along the mainland coast. *In* Paper presented at the Proceedings of the Seventh California Islands Symposium Institute for Wildlife Studies, Arcata, California.

Schroeter, S. C., J. D. Dixon, T. Ebert, and J. Richards. 2019. SBC LTER: Time series of settlement of urchins and other invertebrates. doi:10.6073/pasta/216ce9bcebc219bf7e6380b8d6d30d87

Shanks, A. L. 1983. Surface slicks associated with tidally forced internal waves may transport pelagic larvae of benthic invertebrates and fishes shoreward. Mar. Ecol. Prog. Ser. **13**: 311–315. doi:10.3354/meps013311

Shanks, A. L. 2009. Pelagic larval duration and dispersal distance revisited. Biol. Bull. **216**: 373–385. doi:10.1086/BBLv216n3p373

Shanks, A. L., and G. L. Eckert. 2005. Population persistence of California Current fishes and benthic crustaceans: A marine drift paradox. Ecol. Monogr. **75**: 505–524. doi:10.1890/05-0309

Shanks, A. L., and R. Shearman. 2009. Paradigm lost? Cross-shelf distributions of intertidal invertebrate larvae are unaffected by upwelling or downwelling. Mar. Ecol. Prog. Ser. **385**: 189–204. doi:10.3354/meps08043

Shanks, A. L., S. G. Morgan, J. MacMahan, and A. J. Reniers. 2017. Alongshore variation in barnacle populations is determined by surf zone hydrodynamics. Ecol. Monogr. **87**: 508–532. doi:10.1002/ecm.1265

Shanks, A. L., and S. G. Morgan. 2018. Testing the intermittent upwelling hypothesis: Upwelling, downwelling, and subsidies to the intertidal zone. Ecol. Monogr. **88**: 22–35. doi:10.1002/ecm.1281

Shelton, A. O., and M. Mangel. 2011. Fluctuations of fish populations and the magnifying effects of fishing. Proc. Natl. Acad. Sci. USA **108**: 7075–7080.

Shkedy, Y., and J. Roughgarden. 1997. Barnacle recruitment and population dynamics predicted from coastal upwelling. Oikos **80**: 487–498. doi:10.2307/3546622

Siegel, D., B. Kinlan, B. Gaylord, and S. Gaines. 2003. Lagrangian descriptions of marine larval dispersion. Mar. Ecol. Prog. Ser. **260**: 83–96. doi:10.3354/meps260083

Siegel, D., S. Mitarai, C. Costello, S. Gaines, B. Kendall, R. Warner, and K. Winters. 2008. The stochastic nature of larval connectivity among nearshore marine populations. Proc. Natl. Acad. Sci. USA **105**: 8974–8979.

Strathmann, M. F. 1987. Reproduction and development of marine invertebrates of the northern Pacific coast: Data and methods for the study of eggs, embryos, and larvae. Univ. of Wash. Press.

Strathmann, R. 1978. Length of pelagic period in echinoderms with feeding larvae from the Northeast Pacific. J. Exp. Mar. Biol. Ecol. **34**: 23–27. doi:10.1016/0022-0981(78)90054-0

Sydeman, W. J., E. Poloczanska, T. E. Reed, and S. A. Thompson. 2015. Climate change and marine vertebrates. Science **350**: 772–777. doi:10.1126/science.aac9874

Szuwalski, C. S., K. A. Vert-Pre, A. E. Punt, T. A. Branch, and R. Hilborn. 2015. Examining common assumptions about recruitment: A meta-analysis of recruitment dynamics for worldwide marine fisheries. Fish Fish. **16**: 633–648. doi:10.1111/faf.12083

Tegner, M., and P. Dayton. 1991. Sea urchins, El Niños, and the long term stability of Southern California kelp forest communities. Mar. Ecol. Prog. Ser. **77**: 49–63. doi:10.3354/meps077049

Thorson, J. T., H. J. Skaug, K. Kristensen, A. O. Shelton, E. J. Ward, J. H. Harms, and J. A. Benante. 2015. The importance of spatial models for estimating the strength of

density dependence. Ecology **96**: 1202–1212. doi:10.1890/14-0739.1

Underwood, A., and P. Fairweather. 1989. Supply-side ecology and benthic marine assemblages. Trends Ecol. Evol. **4**: 16–20. doi:10.1016/0169-5347(89)90008-6

Valentine, J. F., and K. Heck Jr. 1999. Seagrass herbivory: Evidence for the continued grazing of marine grasses. Mar. Ecol. Prog. Ser. **176**: 291–302. doi:10.3354/meps176291

Vaughn, D., and J. D. Allen. 2010. The peril of the plankton. Integr. Comp. Biol. **50**: 552–570. doi:10.1093/icb/icq037

Wing, S. R., L. W. Botsford, L. E. Morgan, J. M. Diehl, and C. J. Lundquist. 2003. Inter-annual variability in larval supply to populations of three invertebrate taxa in the northern California Current. Estuar. Coast. Shelf Sci. **57**: 859–872. doi:10.1016/S0272-7714(02)00416-X

Wolter, K., and M. Timlin. 1993. Monitoring ENSO in COADS with a seasonally adjusted principal component index. *In* Paper presented at the Proc. of the 17th Climate Diagnostics Workshop, NOAA/NMC/CAC, NSSL, Oklahoma Clim. Survey, CIMMS and the School of Meteor., Univ. of Oklahoma.

Wolter, K., and M. S. Timlin. 1998. Measuring the strength of ENSO events: How does 1997/98 rank? Weather **53**: 315–324. doi:10.1002/j.1477-8696.1998.tb06408.x

Wong, J. M., K. M. Johnson, M. W. Kelly, and G. E. Hofmann. 2018. Transcriptomics reveal transgenerational effects in purple sea urchins exposed to upwelling conditions, and the response of their progeny to differential pCO_2 levels. Mol. Ecol. **27**: 1120–1137. doi:10.1111/mec.14503

Wong, P. P., I. J. Losada, J.-P. Gattuso, J. Hinkel, A. Khattabi, K. L. McInnes, Y. Saito, and A. Sallenger. 2014. Coastal systems and low-lying areas, p. 361–409. *In* C. B. Field and others. [eds.], Climate change, v. **2104** p. 361–409. Cambridge University Press.

Woodson, C. B., and others. 2012. Coastal fronts set recruitment and connectivity patterns across multiple taxa. Limnol. Oceanogr. **57**: 582–596. doi:10.4319/lo.2012.57.2.0582

Acknowledgments

We are indebted to Tom Ebert and John Dixon, who initiated the larval settlement time series with S.C.S. The Channel Islands Naturalist Corps volunteers, Channel Islands National Park Staff, and Channel Islands long term Kelp Forest Monitoring Program were and remain instrumental in collecting settlement data from Anacapa and benthic data in the Channel Islands. John Richards, Clint Nelson, Shannon Harrer, Jenny Wolf, Peter Kalvass, Brigitte Bondoux, and many students assisted with field collections, laboratory sampling, and data compilation. Sally Holbrook, Russ Schmitt, and Cherie Briggs contributed discussions during initial development of analyses. Kyle Cavanaugh, Dave Siegel, and Tom Bell provided valuable discussions about giant kelp canopy data. Kyle Cavanaugh and Rachel Simons gave important comments on previous manuscript drafts. Funding was provided by the California Urchin Commission, the South Bay Cable Committee, the California Department of Fish and Wildlife Director's Sea Urchin Advisory Committee, and the National Science Foundation's support of the Santa Barbara Coastal Long Term Ecological Research program.

Conflict of Interest

None declared.

Submitted 04 September 2019
Revised 23 January 2020
Accepted 20 February 2020

Associate editor: Ronnie Glud

Supplementary Information - Appendices for "Effects of Ocean Climate on Spatiotemporal Variation in Sea Urchin Settlement and Recruitment"

Daniel K. Okamoto*[1,2], Stephen Schroeter†[3], and Daniel C. Reed‡[3]

[1]Department of Biological Science, Florida State University, Tallahassee, Florida 32303
[2]Ecology, Evolution and Marine Biology, University of California Santa Barbara, Santa Barbara, CA 93106 USA
[3]Marine Science Institute, University of California Santa Barbara, Santa Barbara, CA 93106 USA

*corresponding author: dokamoto@bio.fsu.edu
†email: schroete@lifesci.ucsb.edu
‡email: dan.reed@lifesci.ucsb.edu

Estimation of juvenile urchin densities

The KFM program surveys purple sea urchins at the Santa Barbara Channel Islands by counting the total number of individuals in defined areas and measuring approximately 100 individuals at each site. Thus, to model density we used the number of juveniles measured divided by the total number of individuals measured, multiplied by the total number of individuals counted, divided by the area surveyed:

$$Juvenile \;\; Density_{i,t} = \frac{Juveniles \;\; Measured_{i,t}}{Total \;\; Measured_{i,t}} \frac{Total \;\; Count_{i,t}}{Total \;\; Area_{i,t}}$$

We modeled density in the GLM using the number of measured juvenile urchins (2.5 cm in test diameter- the approximate cutoff size for reproduction - Kenner & Lares 1991). Let represent expected juvenile density at site i in year t. We constructed the regression as:

$$\ln\mu_{i,t} = \alpha_i + \beta \;\; \ln Larval \;\; recruitment_t$$

We allowed the intercept (α_i) to vary by site nested within each island because of overall differences in mean juvenile density among sites and islands. We used a negative binomial (NB) with the using direct mean and variance parameterization form:

$$Juveniles \;\; Measured_{i,t} \sim \text{NB}(\ln\mu_{i,t} - \ln[\frac{1}{TotalMeasured_{i,t}} \frac{TotalCounted_{i,t}}{TotalArea_{i,t}}], \sigma^2)$$

We constructed the model in this format (i.e. with the density denominator in the left hand side of the equation) to maintain the sample size and integer nature of the data while modeling the mean density.

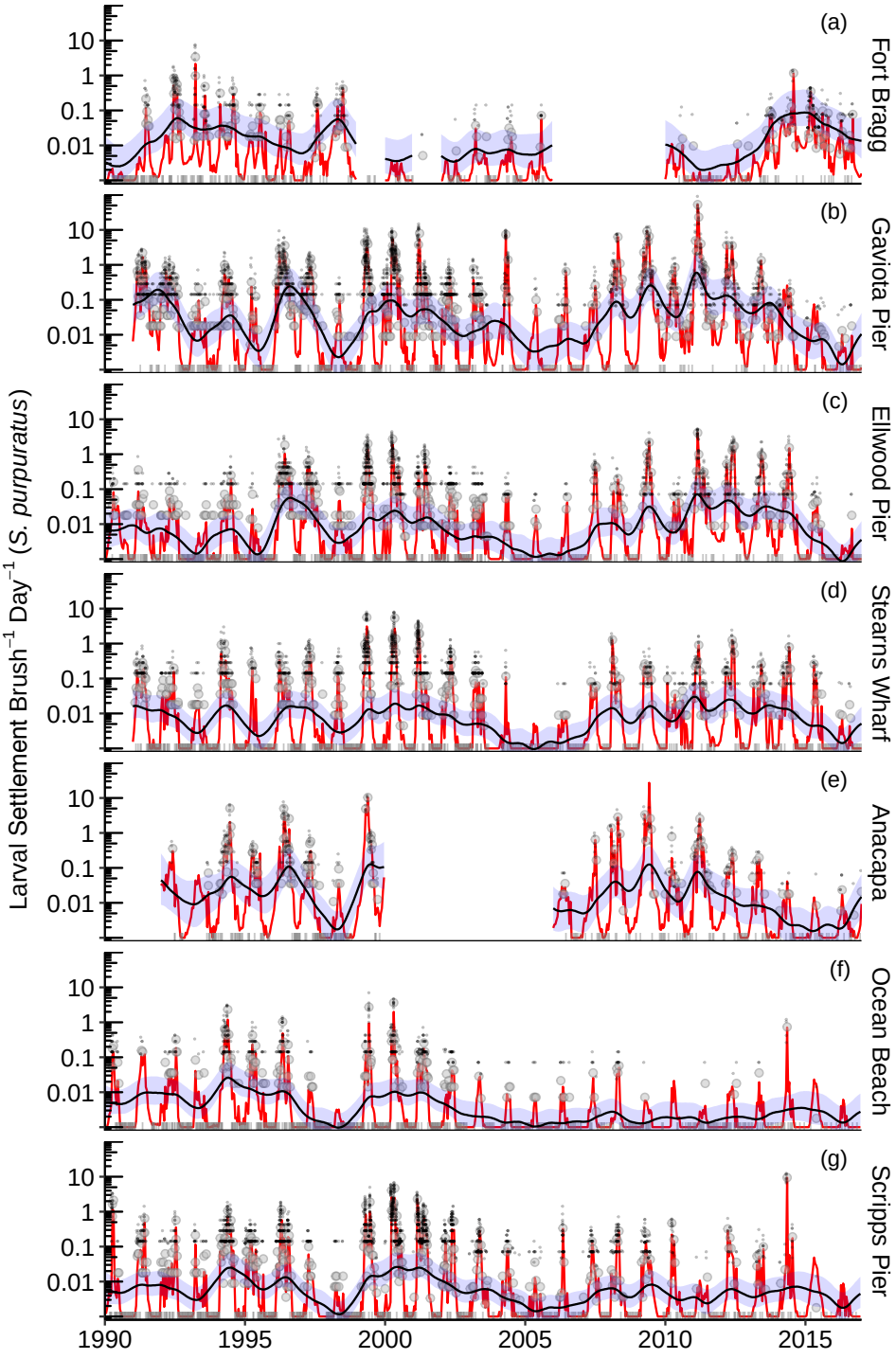

Figure S.1: Observed and estimated purple urchin (*S. purpuratus*) settlement trends from 1990-2016 for each site. Large points represent empirical biweekly means, lines on the axis represent biweekly mean values equal to zero, small points represent counts on individual brushes (only positive values shown for clarity, although the models include zero values), red lines represent biweekly estimates, lines with blue 95% uncertainty intervals represent model estimates of the interannual trends. The model estimates the seasonal trend and the interannual trend at each site simultaneously. For reference, interannual trends for *S. purpuratus* shown here are the unstandardized versions of those shown in Figure 2.

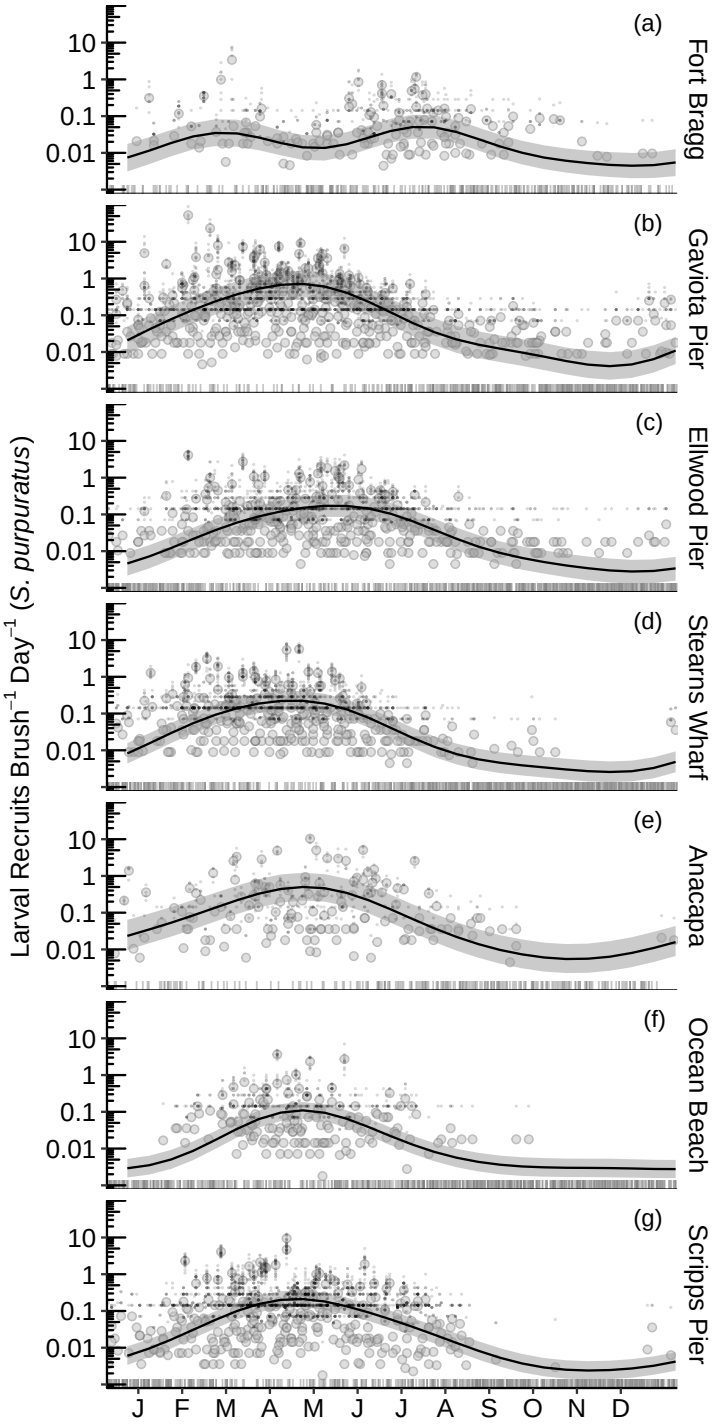

Figure S.2: Seasonal settlement trends from 1990-2016 with the mean estimated seasonal trend for each site. Large points represent empirical biweekly means lines on the axis represent biweekly mean values equal to zero, small points represent counts on individual brushes (only positive values shown for clarity, although the models include zero values), black lines represent the posterior mean and bands represent the 95% uncertainty interval. The model estimates the seasonal trend and the interannual trend at each site simultaneously. For reference, seasonal trends for *S. purpuratus* shown here are the unstandardized versions of those shown in Figure 3.

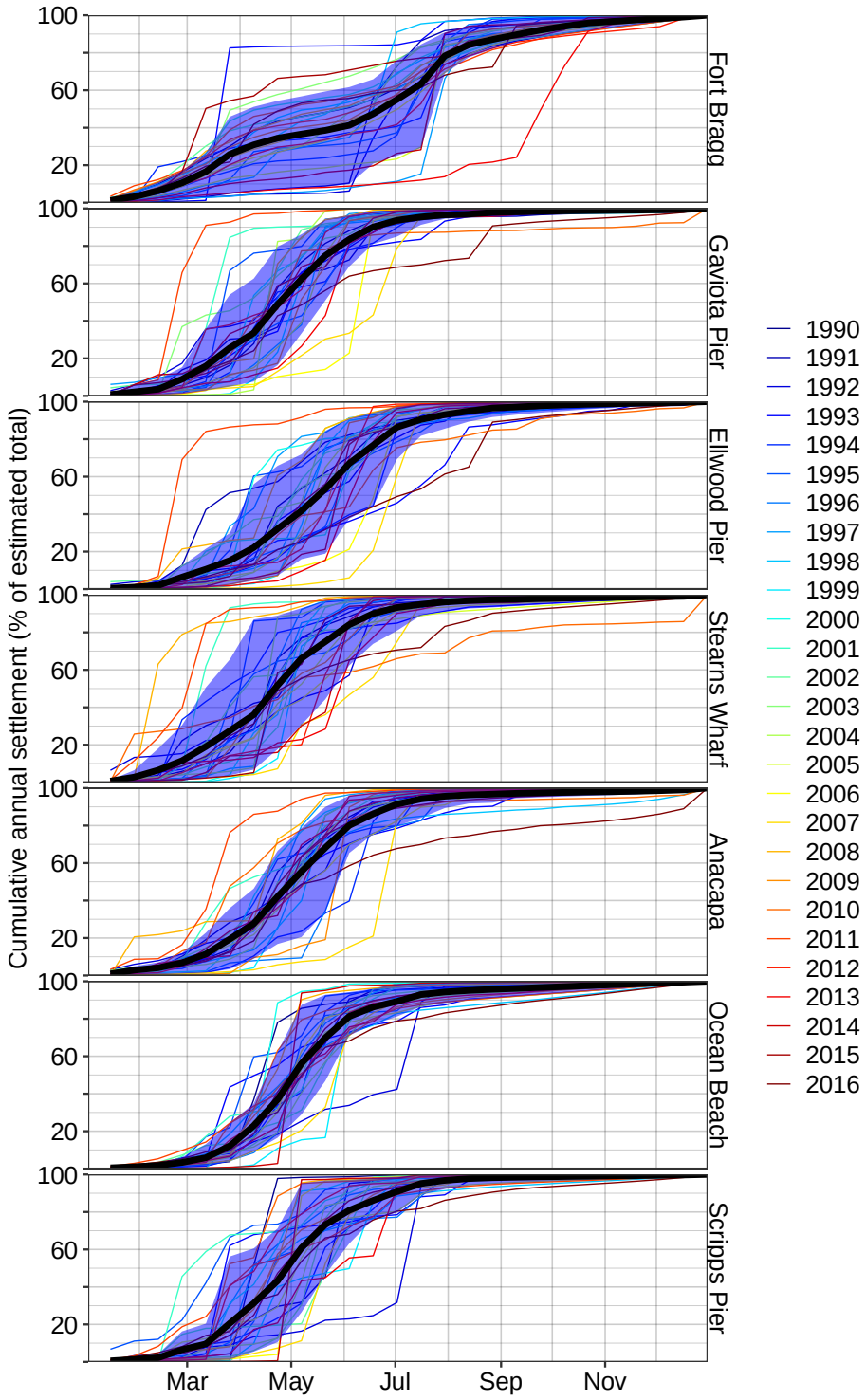

Figure S.3: Cumulative annual mean settlement from the estimated biweekly means for each year. Thick black lines represent the overall mean (i.e. the empirical cumulative mean from Figure 3) and thin, colored lines represent the cumulative annual values of the red lines in Figure S1. Blue bands represent the 10 and 90% quantiles for each biweekly period.

Variable Correlations

To illustrate the intercorrelated nature of the covariates and responses, we estimated a network model for Gaviota Pier that includes the independent model estimates of *S. purpuratus* settlement and its seasonality. To do so, we first constrained network structure by excluding all nonsensical interactions (i.e. chlorophyll does not cause ENSO events and is thus eliminated a priori) and including all known directional interactions (i.e. estimated seasonality affecting settlement for is forced into the network). Learning of the network skeleton is achieved via the Hill Climbing algorithm using the bnlearn (Scutari 2010) package in R. Note that strong collinearity can result in the weaker correlation being ignored (e.g. ENSO over SST with Larval Recruitment).

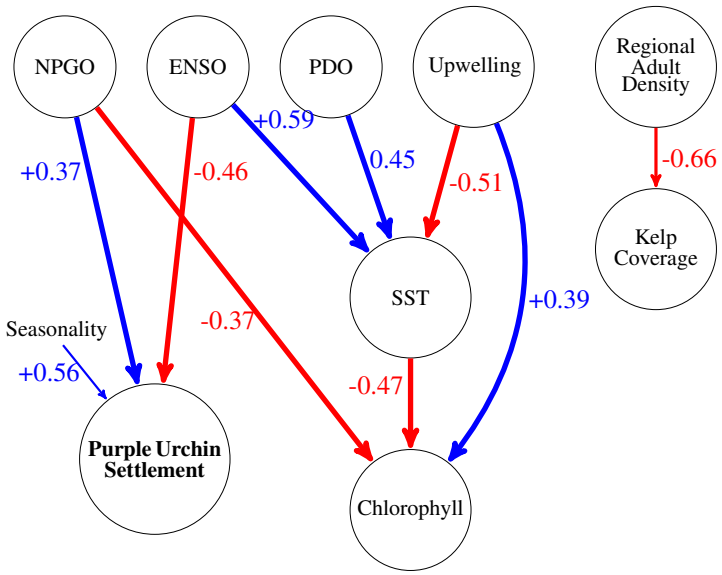

Figure S.4: Bayesian network model structure inferred for the Santa Barbara Channel. Numbers represent the partial correlation coefficients accounting for all other variables pointing to that node. All correlations shown are significant at alpha= 0.05

References

Kenner M. & Lares M. (1991) Size at first reproduction of the sea urchin *Strongylocentrotus purpuratus* in a central California kelp forest. Mar Ecol Prog Ser, 76, 303-306

Lewandowski D., Kurowicka D. & Joe H. (2009) Generating random correlation matrices based on vines and extended onion method. J Multivar Anal, 100, 1989-2001

MacKay D.J. (1998) Introduction to Gaussian processes. NATO ASI Series F Computer and Systems Sciences, 168, 133-166

Polson N.G. & Scott J.G. (2012) On the half-Cauchy prior for a global scale parameter. Bayesian Analysis, 7, 887-902

Rasmussen C.E. & Williams C.K.I. 2006. Gaussian Processes for Machine Learning. The MIT Press, Cambridge, Massachusetts

Scutari M. (2010). Learning Bayesian Networks with the bnlearn R Package. Journal of Statistical Software, 35(3), 1-22. URL http://www.jstatsoft.org/v35/i03/

```
\\\\\\\\\\\\\\\\\\\\\\\\\\\\\\\\\\\\\\\\\\\\\\\\\\\\\\\\\\\\
\\ Stan Code Required to Estimate Trends     \\
\\ Author: D.K. Okamoto                      \\
\\\\\\\\\\\\\\\\\\\\\\\\\\\\\\\\\\\\\\\\\\\\\\\\\\\\\\\\\\\\

data {
  // input information
  int NO; // number of observations
  int NS; // number of sites
  int NM; // number of months
  int NYM; // number of months
  int NSUB; // number of observations with subsamples
  // input data
  //  Beta priors for uncertainty in subsamples
  vector[NSUB] P1; // SP observations (on the original scale)+0.5
  vector[NSUB] P2; // SP observations - subsample count (on the original scale) +
      0.5
  int SUB[NSUB];

  int N[NO]; // total count (on the original scale)
  int OBS[NO]; // continuous month-site observation index
  int PRED_MONTH[NM]; // month-site observation index associated with MA
  vector[NO] D; // number of days
  cholesky_factor_cov[NYM] D_seas;   // seasonal cholesky covariance factor
  cholesky_factor_cov[NM] D_ann;   // annual cholesky covariance factor
}

parameters {
  // mean volatility
  vector<lower=1e-7>[NS] sigma_S_mu;

  // spatial volatility correlation matrix
  cholesky_factor_corr[NS] L_Omega_S; //
  cholesky_factor_corr[NS] L_Omega_Spatial;

  // seasonal and annual variance
  vector<lower = 0>[NS] sigma;
  vector<lower = 0>[NS] sigma2;

  // mean site settlement
  row_vector<lower= -10, upper= 10>[NS] mu_S;

  // iid errors for seasonality
  matrix<lower= -10, upper= 10>[NYM,NS] z_s;

  // iid errors for annual trends
  matrix<lower= -10, upper= 10>[NS,NM] w_z;

  // iid errors for residuals
  matrix<lower= -4, upper= 4>[NS,NM] e_z;

  // proportion of samples that are purps
  vector<lower= 0,upper= 1>[NSUB] theta;
}

transformed parameters {
  matrix[NYM,NS] LS; // log scale expected sp per brush, per day for every month

  matrix[NM,NS] S; // estimated abundance
```

```
  vector[NO] S_exp; // normal scale estimated sp for each observation

  vector[NO] theta2; // fraction that is SP

  matrix[NM,NS] w;

  // correlated errors
  matrix[NM,NS] e;

  LS  = D_seas*z_s;
  w = D_ann*transpose(L_Omega_Spatial*w_z);

  theta2 = rep_vector(1.0,NO);
  theta2[SUB] = theta;
  // put it all together
  e = transpose(diag_pre_multiply(sigma_S_mu,L_Omega_S)*e_z);
  S= rep_matrix(mu_S,NM)+diag_post_multiply(LS[PRED_MONTH,],sigma2)+
      diag_post_multiply(w,sigma)+e;
  S_exp = exp(to_vector(S)[OBS]) .*D ./theta2;
}

model {
  sigma ~ cauchy(0, 0.5);
  sigma2 ~ cauchy(0, 0.5);

  L_Omega_S ~ lkj_corr_cholesky(2);
  L_Omega_Spatial ~ lkj_corr_cholesky(2);

  for(i in 1:NS){
    z_s[i]~ normal(0,1);
    mu_S[i] ~ normal(0,5);
  }

  sigma_S_mu ~ cauchy(0,2.5);

  // uncertainty on proportions of purples in the sample
  // jeffrey's prior given subsampling
  theta~beta(P1, P2);

  // observation likelihood
  N~poisson(S_exp);
}
```

```
\\\\\\\\\\\\\\\\\\\\\\\\\\\\\\\\\\\\\\\\\\\\\\\\\\\\\\\\\\\\\\\\\\\\
\\ Stan Code Required to Estimate Bayesian Regression \\
\\ Author: D.K. Okamoto                                \\
\\\\\\\\\\\\\\\\\\\\\\\\\\\\\\\\\\\\\\\\\\\\\\\\\\\\\\\\\\\\\\\\\\\\
data {
  // input information
  int NO; // number of observations
  int NS; // number of sites
  int NM; // number of months
  int NYM; // number of months
  int NSUB; // number of observations with subsamples
  int NSP; // number of subsample counts
  int NP; // number of variables
  // input data
  //  Beta priors for uncertainty in subsamples
  vector[NSP] P1; // SP observations (on the original scale)+0.5
  vector[NSP] P2; // NON SP observations (on the original scale) + 0.5
  int SUB[NSUB];
  int ID[NO];
  int OBS[NO]; // continuous month-site observation index
  // input data
  int N[NO]; // total count (on the original scale)
  int OBS_MONTH[NO]; // continuous month-site observation index associated with MA
  int OBS_SITE[NO]; // month-site observation index associated with MA
  int PRED_MONTH[NM]; // month-site observation index associated with MA
  matrix[NM*NS,NP] X; // covariate matrix
  int xind[NM,NS]; // covariate matrix indices
  vector[NO] D; // number of days
  cholesky_factor_cov[NYM] D_seas;   // seasonal cholesky covariance factor
  real<lower= 0> m0;
  real<lower= 0> sigma_scale;
  real<lower= 0> slab_scale;
}

parameters {
  // mean volatility
  vector<lower=0>[NS] sigma_S_mu;

  // spatial volatility correlation matrix
  cholesky_factor_corr[NS] L_Omega_S; //
  cholesky_factor_corr[NS] L_Omega_Spatial_seas;

  // iid errors for seasonality
  matrix[NYM,NS] z_s;

  // seasonal and annual variance
  real<lower = 0> sigma[NS];

   // mean site settlement
  row_vector[NS] mu_S;

  // iid errors for residuals
  matrix<lower= -4,upper=4>[NS,NM] e_z;

  // AR1 parameters
  vector<lower= -0.9,upper= 0.9>[NS] phi;

  // proportion of samples that are purps
  vector<lower= 0,upper= 1>[NSP] theta;
```

```
  // iid errors for seasonal gaussian process
  vector[NP] beta_tilde;
  vector<lower=0>[NP] lambda;
  real<lower=0> c2_tilde;
  real<lower=0> tau_tilde;
  real alpha;
}

transformed parameters {
  matrix[NYM,NS] LS; // log scale expected sp per brush, per day for every month
  matrix[NM,NS] S; // estimated abundance
  vector[NO] S_exp; // normal scale estimated sp for each observation

  vector[NO] N_mu; // expected total count
  vector[NO] q_mu; // expected fraction of N that is SP
  vector[NS] sigma_star;

  vector[NM*NS] s_hat;

  // process variables
  vector[NO] theta2; // fraction that is SP

  // correlated errors
  matrix[NM,NS] e;
  matrix[NM,NS] e_hat;

  vector[NP] beta;
  vector[NP] lambda_tilde;

  real tau0 = (m0/(NP-m0))*(mean(sigma_S_mu)*sqrt(1.0*NM*NS));
  real slab_scale2 = square(slab_scale);
  real half_slab_df = 0.5 * 25;

  real tau = tau0 * tau_tilde;
  real c2 = slab_scale2 * c2_tilde;
  lambda_tilde  = sqrt( c2 * square(lambda) ./ (c2 + square(tau) * square(lambda))
      );
  beta = tau * lambda_tilde .* beta_tilde;

  // regression model
  s_hat = X*beta;

  // seasonal gaussian process model
  LS  = D_seas*z_s;

  // process error
  for(i in 1:NS){
    sigma_star[i] = sigma_S_mu[i]*sqrt(1.0-phi[i]^2.0);
  }
  e = transpose(diag_pre_multiply(sigma_star,L_Omega_S)*e_z);
  // put it all together

  for(j in 1:NS){
    e_hat[1,j] = e[1,j];
    S[1,j]=mu_S[j]+LS[PRED_MONTH[1],j]*sigma[j]+s_hat[xind[1,j]]+e_hat[1,j]-5;
    for(i in 2:NM){
      e_hat[i,j] =  phi[j]*e_hat[i-1,j]+e[i,j];
      S[i,j]=mu_S[j]+LS[PRED_MONTH[i],j]*sigma[j]+s_hat[xind[i,j]]+e_hat[i,j]-5;
```

```
    }
  }

  theta2 = rep_vector(1.0,NO);
  theta2[SUB] = theta[ID[SUB]];

  S_exp = exp(to_vector(S)[OBS]) .*D ./theta2;
}

model {
  sigma ~ normal(0.0, 2);

  L_Omega_S ~ lkj_corr_cholesky(2.0);

  for(i in 1:NS){
    z_s[i]~ normal(0.0,1.0);
    e_z[i]~ normal(0.0,1.0);
    mu_S[i] ~ cauchy(0.0,10);
  }

  sigma_S_mu ~ normal(0.0,sigma_scale);

  beta_tilde ~ normal(0, 1);
  lambda ~ cauchy(0, 1);
  tau_tilde ~ cauchy(0, 1);
  c2_tilde ~ inv_gamma(half_slab_df, half_slab_df);

  // jeffrey's prior given subsampling
  theta~beta(P1, P2);

  // observation likelihood
  N~poisson(S_exp);
}
```

Supplementary Information - Appendices for "Effects of Ocean Climate on Spatiotemporal Variation in Sea Urchin Settlement and Recruitment"

Daniel K. Okamoto*[1,2], Stephen Schroeter†[3], and Daniel C. Reed‡[3]

[1]Department of Biological Science, Florida State University, Tallahassee, Florida 32303
[2]Ecology, Evolution and Marine Biology, University of California Santa Barbara, Santa Barbara, CA 93106 USA
[3]Marine Science Institute, University of California Santa Barbara, Santa Barbara, CA 93106 USA

*corresponding author: dokamoto@bio.fsu.edu
†email: schroete@lifesci.ucsb.edu
‡email: dan.reed@lifesci.ucsb.edu